Title

Septin Dynamics Are Essential for Exocytosis*

Journal

Journal of Biological Chemistry, 290(9)

ISSN

0021-9258

Authors

Tokhtaeva, Elmira

Capri, Joe

Marcus, Elizabeth A

et al.

Publication Date

2015-02-01

DOI

10.1074/jbc.m114.616201

Peer reviewed

THE JOURNAL OF BIOLOGICAL CHEMISTRY VOL. 290, NO. 9, pp. 5280–5297, February 27, 2015
Published in the U.S.A.

Septin Dynamics Are Essential for Exocytosis*

Received for publication, October 3, 2014, and in revised form, January 5, 2015 Published, JBC Papers in Press, January 9, 2015, DOI 10.1074/jbc.M114.616201

Elmira Tokhtaeva[‡§], Joe Capri[¶], Elizabeth A. Marcus[§‖], Julian P. Whitelegge[¶], Venera Khuzakhmetova[‡‡], Ellya Bukharaeva[**‡‡], Nimrod Deiss-Yehiely[§§], Laura A. Dada[§§], George Sachs[‡§], Ester Fernandez-Salas[¶¶], and Olga Vagin[‡§1]**

*From the Departments of [‡]Physiology and [‖]Pediatrics, David Geffen School of Medicine at UCLA, Los Angeles, California 90095, [§]Veterans Affairs Greater Los Angeles Healthcare System, Los Angeles, California 90073, [¶]The Neuropsychiatric Institute-Semel Institute, Pasarow Mass Spectrometry Laboratory, UCLA, Los Angeles, California 90024, **Kazan Institute of Biochemistry and Biophysics, Kazan Scientific Center of the Russian Academy of Sciences, Kazan 420111, Russia, [‡‡]Kazan Federal University, Kazan 420008, Russia, [§§]Division of Pulmonary and Critical Care Medicine, Feinberg School of Medicine, Northwestern University, Chicago, Illinois 60611, and [¶¶]Department of Pathology, School of Medicine, University of Michigan, Ann Arbor, Michigan 48109*

Background: Septins serve as scaffolds for membrane-associated protein complexes.
Results: Knockdown of septin-2 or disruption of septin assembly/disassembly impairs interactions between exocytic proteins and inhibits late steps of exocytosis.
Conclusion: Septins undergo dynamic reorganization to facilitate localized and timely interactions between exocytosis-essential proteins.
Significance: Both the presence of septin-2 and active reorganization of septin oligomers are required for exocytosis.

Septins are a family of 14 cytoskeletal proteins that dynamically form hetero-oligomers and organize membrane microdomains for protein complexes. The previously reported interactions with SNARE proteins suggested the involvement of septins in exocytosis. However, the contradictory results of up- or down-regulation of septin-5 in various cells and mouse models or septin-4 in mice suggested either an inhibitory or a stimulatory role for these septins in exocytosis. The involvement of the ubiquitously expressed septin-2 or general septin polymerization in exocytosis has not been explored to date. Here, by nano-LC with tandem MS and immunoblot analyses of the septin-2 interactome in mouse brain, we identified not only SNARE proteins but also Munc-18-1 (stabilizes assembled SNARE complexes), *N*-ethylmaleimide-sensitive factor (NSF) (disassembles SNARE complexes after each membrane fusion event), and the chaperones Hsc70 and synucleins (maintain functional conformation of SNARE proteins after complex disassembly). Importantly, α-soluble NSF attachment protein (SNAP), the adaptor protein that mediates NSF binding to the SNARE complex, did not interact with septin-2, indicating that septins undergo reorganization during each exocytosis cycle. Partial depletion of septin-2 by siRNA or impairment of septin dynamics by forchlorfenuron inhibited constitutive and stimulated exocytosis of secreted and transmembrane proteins in various cell types. Forchlorfenuron impaired the interaction between SNAP-25 and its chaperone Hsc70, decreasing SNAP-25 levels in cultured neuroendocrine cells, and inhibited both spontaneous and stimulated acetylcholine secretion in mouse motor neurons. The results demonstrate a stimulatory role of septin-2 and the dynamic reorganization of septin oligomers in exocytosis.

Membrane fusion is essential for intracellular vesicular trafficking and exocytosis in all eukaryotic cells, including synaptic exocytosis in neurons. Membrane fusion is promoted by universal machinery that involves soluble *N*-ethylmaleimide-sensitive factor (NSF)[2] attachment protein receptor (SNARE) proteins (1, 2). During membrane fusion, vesicular and target SNARE proteins assemble into the trans-SNARE complex that brings the two membranes together, whereas Munc-18-1-like proteins interact with the newly assembled trans-SNARE complexes to facilitate membrane fusion (3). After fusion, SNARE complexes are dissociated by the ATPase NSF, which allows vesicle SNARE endocytosis and a repeat of the subsequent membrane fusion events (4). Fusion-competent conformations of SNARE proteins after disassembly are maintained by chaperone complexes composed of cysteine string protein α (Dnajc5), Hsc70 (Hspa8), and small glutamine-rich tetratricopeptide repeat-containing, α (Sgta) and by non-enzymatically acting synuclein chaperones (1, 5, 6).

Septins are GTP-binding proteins that form hetero-oligomeric complexes and higher order structures, including filaments and rings, and have been recently recognized as a component of the cytoskeleton (7). Fourteen human isoforms of septins have been identified to date (8). Recent studies have

* This work was supported, in whole or in part, by National Institutes of Health Grants R01HL113350 from the NHLBI (to L. A. D. and O. V.), UL1TR000124 (to the UCLA *Clinical and Translational Science Institute* and E. A. M.), and K08DK100661-01 (to E. A. M.) and P30DK063491 from the NIDDK (to J. P. W.). This work was also supported by the UCLA *Children's Discovery and Innovation Institute* (to E. A. M.), the Program of Competitive Growth of Kazan Federal University (to E. B. and V. K.), and Russian Foundation for Basic Research Grant 15-04-02983a (to E. B. and V. K.).

[1] To whom correspondence should be addressed: Dept. of Physiology and Medicine, UCLA, 11301 Wilshire Blvd., VAGLAHS/West LA, Bldg. 113, Rm. 324, Los Angeles, CA 90073. Tel.: 310-478-3711 (ext. 42055); Fax: 310-312-9478; E-mail: olgav@ucla.edu.

[2] The abbreviations used are: NSF, *N*-ethylmaleimide-sensitive factor; FCF, forchlorfenuron; DPPIV, dipeptidyl peptidase 4; sec-β1, a chimeric protein between DPPIV and the extracellular domain of the Na,K-ATPase β_1 subunit; EPC, endplate current; SNAP, soluble NSF attachment protein; nLC-MS/MS, nano-LC with tandem MS; MDCK, Madin-Darby canine kidney; ER, endoplasmic reticulum; EndoH, endoglycosidase H.

implicated septins in numerous cellular processes and signaling pathways (7, 9, 10). Co-purification and co-immunoprecipitation of septins with the exocyst complex, which mediates the tethering of secretory vesicles to the plasma membrane (11, 12), suggested a possible involvement of septins in targeting vesicles to exocytic sites (13). Several reports on localization of septins in the presynaptic membrane in neurons (14–18), interaction of septins with SNARE proteins (17, 19–24), and aberrant exocytosis in cells with altered levels of expression of septin-4 or septin-5 (16, 17, 24) suggested a role for septins in membrane fusion and secretion of neurotransmitters into the synaptic cleft. However, the results on the role of septins in exocytosis are controversial. Mice lacking septin-5 displayed enhanced platelet secretion (24) and enhanced neurotransmission in the immature calyx of Held synapses (16), suggesting a role for septin-5 in suppressing exocytosis. By contrast, mice lacking septin-4 exhibited diminished dopaminergic neurotransmission (17), suggesting that septin-4 promotes exocytosis. Mice lacking septin-3 or septin-6 had normal neurotransmission (25, 26). The involvement of other septins, including the ubiquitously expressed septin-2, in exocytosis has not been examined.

The interpretation of the effects of knocking out particular septins in the whole animal on exocytosis might be misleading given the possibility of functional redundancy and compensatory mechanisms by other septins. Here, to elucidate the role of septins in exocytosis, we used acute down-regulation of the major ubiquitously expressed septin, septin-2, by transient siRNA. In addition, we used the inhibitor of septin organization, forchlorfenuron (FCF), which specifically impairs assembly and disassembly of septin hetero-oligomers (27–29) without affecting actin or tubulin polymerization (27, 30). Both FCF and knockdown of septin-2 decreased the rate of exocytosis in cultured cells. By nano-liquid chromatography with tandem mass spectrometry (nLC-MS/MS) and Western blot analyses of the septin-2 interactome, we have identified not only other septins and SNARE proteins as interacting partners but also NSF, Munc-18-1, synucleins, and Hsc70 and found that FCF impaired the interactions of these proteins with each other and with septins. In addition, FCF inhibited both spontaneous and stimulated secretion of neurotransmitters by mouse motor neurons. The results demonstrate the importance of septin-2 and septin dynamics for exocytosis.

EXPERIMENTAL PROCEDURES

Primary Antibodies—A polyclonal antibody against septin-2 (Sigma-Aldrich) and a monoclonal antibody against SNAP-25, clone 71.1 (Synaptic System, Gottingen, Germany), were used for immunoprecipitation. The following monoclonal antibodies were used for Western blot analysis: against the Na,K-ATPase β_1 subunit, clone 464.8 (Novus Biologicals, Littleton, CO); NSF, clone NSF-1 and actin (EMD Millipore, Temecula, CA), SNAP-25, clone SP-12, horseradish peroxidase-conjugated (LifeSpan BioSciences, Inc., Seattle, WA); Hsc70 (HSPA8), clone 1B5 (Pierce); α-SNAP, clone 4E4 and syntaxin-1, clone HPC-1 (Sigma-Aldrich); β-synuclein, clone EP1537Y (Novus Biologicals, Littleton, CO); RIG-1 (DDX58 (8D2)) (Abcam, Cambridge, MA); and interleukin 6 (IL-6) (Millipore, Temecula, CA). The following polyclonal antibodies were used for Western blot analysis: septin-7 (H-120) (Santa Cruz Biotechnology, Inc., Santa Cruz, CA), septin-2 and septin-9 (Sigma-Aldrich), and β-actin (Cell Signaling Technology, Inc., Danvers, MA).

Cell Culture—HEK-293, MDCK, or A549 cells (ATCC, Manassas, VA) and HGT-1 cells (31) were grown in DMEM (Cellgro Mediatech, Manassas, VA) containing 4.5 g/liter glucose, 2 mM L-glutamine, 8 mg/liter phenol red, 100 units/ml penicillin, 0.1 mg/ml streptomycin, and 10% FBS. A549 cells stably expressing Na,K-ATPase α_1 subunit tagged with GFP (32) were grown in the medium supplemented with 3 μM ouabain (ICN Biomedicals Inc., Aurora, OH) to suppress endogenous Na,K-ATPase α_1 subunit. The MDCK stable cell line expressing YFP-tagged bile acid transporter and HEK-293 stable cell line expressing YFP-tagged Na,K-ATPase β_1 subunit were constructed as described previously (33). HGE-20 cells (34) were grown in 50:50 DMEM:F-12 (Invitrogen) with 10% FBS, 100 units/ml penicillin, and 0.1 mg/ml streptomycin. HGE-20 cells, a derivative of the NCI-N87 gastric carcinoma cell line, were provided by Dr. Daniel Mènard, who kindly granted permission to use the cells for this work. Rat pheochromocytoma PC12 cells (ATCC, Manassas, VA) were grown in RPMI 1640 medium with 2 mM GlutaMAX™, 10 mM HEPES, 1 mM sodium pyruvate, 100 units/ml penicillin, and 100 μg/ml streptomycin (Sigma-Aldrich) supplemented with 10% FetalPlex animal serum complex (Gemini Bio-Products, West Sacramento, CA).

Immunoprecipitation—Cells were rinsed twice with ice-cold PBS and lysed by incubation with 50 mM Tris, pH 7.5 containing 150 mM NaCl, 1% Nonidet P40, 0.5% sodium deoxycholate, and Complete protease inhibitor mixture (1 tablet/50 ml; Roche Diagnostics) at 4 °C for 30 min. Cells were scraped from the plates, and cell extracts were clarified by centrifugation (15,000 × *g* for 10 min) at 4 °C. Mouse brain was homogenized, cell debris was removed by centrifugation (2,000 × *g* for 10 min), and proteins were extracted by incubation of the supernatant with 50 mM Tris, pH 7.5 containing 1% *n*-dodecyl β-D-maltoside and Complete protease inhibitor mixture (1 tablet/50 ml) at 4 °C for 30 min. Membrane extracts were clarified by centrifugation (100,000 × *g* for 1 h) at 4 °C. Septin-2 or SNAP-25 was immunoprecipitated from total cell lysates (1–2 mg of protein) or mouse brain extracts (0.5–1 mg of protein) by using 2 μl of an appropriate antibody as described previously (35). Protein A-agarose suspension (Roche Diagnostics) was used for immunoprecipitation with rabbit polyclonal septin-2 antibodies, whereas protein G-agarose suspension (Roche Diagnostics) was used for immunoprecipitation with mouse monoclonal SNAP-25 antibodies. The adherent proteins were eluted from the beads by incubation in 35 μl of SDS-PAGE sample buffer (4% SDS, 0.05% bromphenol blue, 20% glycerol, 1% β-mercaptoethanol in 0.1 M Tris, pH 6.8) for 5 min at 80 °C.

Deglycosylation of a Chimeric Protein between Dipeptidyl Peptidase 4 (DPPIV) and the Extracellular Domain of the Na,K-ATPase β_1 Subunit (Sec-β1)—Deglycosylation of sec-β1 present in cell lysates or culture media was performed by using peptide *N*-glycosidase F from *Flavobacterium meningosepticum* (New England Biolabs Inc., Ipswich, MA) or endoglycosi-

dase H from *Streptomyces plicatus* (Glyco-Prozyme Inc., Hayward, CA) according to the manufacturers' instructions.

Immunofluorescence Staining—Fixation and immunostaining of cells grown in glass bottom dishes (MatTek Corp., Ashland, MA) were performed as described previously (36) using a polyclonal antibody against septin-2 or septin-9 (Sigma-Aldrich) and Alexa Fluor 633-conjugated anti-rabbit IgG secondary antibodies (Invitrogen).

Confocal Microscopy and Image Analysis—Confocal microscopy images were acquired using a Zeiss LSM 510 laser-scanning confocal microscope (Carl Zeiss MicroImaging GmbH, Germany) using appropriate laser settings. Confocal microscopy images were analyzed using ZEN 2009 software (Carl Zeiss MicroImaging GmbH). To quantify the intracellular accumulation of vesicles, the ratio between the intracellular fluorescence intensity and the total cellular fluorescence intensity was calculated. At least 10 confocal microscopy images per condition were analyzed for each of the three independent experiments. At least five cells were analyzed on each image. To quantify the alterations in septin organization caused by septin-2 siRNA or FCF, the percentage of cells containing continuous septin-2- or septin-9-positive structures that are longer than 2 μm was calculated by analyzing at least 10 confocal microscopy images per condition for each of the three independent experiments. The threshold of 2 μm was chosen arbitrarily based on the observation that in the majority of untreated cells the size of continuous septin-positive structures was smaller than 2 μm. Each image contained at least 20 cells.

Protein Secretion Assay—HEK-293 cells were transiently transfected with the vector encoding the chimera containing 29 N-terminal amino acid residues (comprising a cytoplasmic and a transmembrane domain) of DPPIV and amino acid residues 64–303 (extracellular domain) of the dog Na,K-ATPase β_1 subunit. This vector, which was constructed by Maura Hamrick in Dr. Douglas Fambrough's laboratory, was a generous gift from Dr. Liora Shoshani. The single L28A amino acid substitution in the DPPIV portion of this chimera generated a cleavage site for the endoplasmic reticulum (ER) signal peptidase, resulting in secretion of the soluble protein sec-β1 that corresponds to the extracellular domain of the Na,K-ATPase β_1 subunit (37, 38). To determine the rate of secretion, aliquots of the culture medium were collected at the indicated time periods, and the amount of accumulated sec-β1 was determined by Western blot analysis. To control for the number of secreting cells and for the level of sec-β1 expression, the amount of sec-β1 in the medium was compared with the total amount in cell lysates. The antibody used for Western blot analysis reacts with the extracellular domain of the dog, but not human, Na,K-ATPase β_1 subunit (38), resulting in specific detection of sec-β1 without cross-reaction with the endogenous Na,K-ATPase β_1 subunit in HEK-293 cell lysates.

Knockdown of Proteins in HEK-293 Cells—Expression of septin-2 was knocked down by using a mixture of two Ambion predesigned siRNA duplexes: sense, 5′-GAAAAUCGACUCUCAUAAATT-3′ and antisense, 5′-UUUAUGAGAGUCGAUUUUCCT-3′ (duplex 1) and sense, 5′-CAAUCAAGUUCACCGAAAATT-3′ and antisense, 5′-UUUUCGGUGAACUUGAUUGGG-3′ (duplex 2) (Invitrogen). Knockdown of NSF was performed using the SMARTpool ON-TARGETplus Human NSF (4905) siRNA (Thermo Scientific, Pittsburgh, PA). A mixture of equal amounts of two individual siGENOME siRNAs, 5′-GAAGGUGGCUGGUUACGCU (duplex 1) and 5′-CAGAGUUGGUGGACAUCGA (duplex 2) (Thermo Scientific, Pittsburgh, PA) was used to down-regulate α-SNAP expression. The Ambion Silencer® Negative Control Number 1 siRNA (Invitrogen), was used as a negative control. HEK-293 cells in a 6-well plate (50% confluent) were transfected with siRNA using Lipofectamine 2000 transfection reagent (Invitrogen) according to the manufacturers' protocols. 48 h after the first transfection, cells were transfected again with the mixture of the siRNA that was used in the first transfection and the plasmid that encodes for sec-β1. Cells were used in the secretion assay 24 h after the second transfection.

For the time course experiments with cycloheximide, to ensure equal expression levels of sec-β1 in multiple wells, HEK-293 cells were transfected in suspension with the plasmid that encodes for sec-β1 and then seeded in three 6-well plates. 16 h later, the cells in one of these plates were transfected with septin-2 siRNA, whereas the cells grown in two other plates were transfected with negative control siRNA. Cells were used in the time course experiment 24 h after siRNA transfection.

For imaging experiments, non-transfected HEK-293 cells or HEK-293 cells expressing the YFP-tagged Na,K-ATPase β_1 subunit grown on glass bottom dishes (MatTek Corp.) were transfected with the indicated siRNA. 24 h after transfection with siRNA, cells were either analyzed by confocal microscopy or fixed for the following immunofluorescence staining of septins. Where indicated, 8 h after the first transfection, cells were additionally transfected with the plasmid encoding a fluorescent ER marker, DsRed2-ER (Clontech).

Western Blot Analysis—Immunoprecipitated proteins eluted from the beads and cell lysates were separated by SDS-PAGE, transferred onto nitrocellulose membranes (Bio-Rad), and detected by Western blot analysis as described previously (38). Immunoblots were quantified by densitometry using Image Studio Software (LI-COR Inc., Lincoln, NE).

nLC-MS/MS of Immunoprecipitated Proteins—To analyze proteins co-immunoprecipitated with septin-2 by nLC-MS/MS, immunoprecipitation was performed as described above. Proteins were eluted from the beads by incubation in 35 μl of SDS-PAGE sample buffer for 5 min at 80 °C and separated by SDS-PAGE using 4–12% gradient reducing gels. Each lane was excised and sliced into 12 pieces horizontally. Proteins contained in each gel slice were enzymatically cleaved overnight at 37 °C with 50 ng of trypsin (Promega, Madison, WI) and extracted from the gel with acetonitrile. Extracted peptides were desalted using C_{18} StageTips (39) and analyzed by nLC-MS/MS with collision-induced dissociation. This was performed on an Orbitrap XL mass spectrometer (Thermo Scientific, Waltham, MA) integrated with an Eksigent 2D nano-LC system. A prepacked reverse-phase C_{18} 75-μm × 20-cm column containing C_{18} 5-μm-particle size, 300-Å-pore size resin (Acutech Scientific, San Diego, CA) was used for peptide chromatography and subsequent collision-induced dissociation analyses. Electrospray ionization conditions using a nanospray source (Thermo Fisher Scientific, Waltham, MA) for the

Orbitrap were set as follows: capillary temperature of 210 °C, tube lens voltage of 125 V, and spray voltage of 2.3 kV. The flow rate for reverse-phase chromatography was 500 nl/min for loading and analytical separation (buffer A, 0.1% formic acid, 3% acetonitrile; buffer B, 0.1% formic acid, 100% acetonitrile). Peptides were resolved by a linear gradient of 3–40% buffer B over 180 min. The LTQ Orbitrap was operated in data-dependent mode with a full precursor scan at high resolution (60,000 at m/z 400) and 10 MS/MS experiments at low resolution on the linear trap while the full scan was completed. For collision-induced dissociation, the intensity threshold was set to 500 where the mass range was 350–2,000. Dynamic exclusion was set to a repeat count of 1, repeat duration of 30 s, and exclusion duration of 30 s. Spectra were searched using Mascot software (v2.4, Matrix Science, UK) in which results with $p < 0.05$ (95% confidence interval) were considered significant, indicating identity.

Measurements of the Synaptic Secretion of Acetylcholine—Experiments were performed on phrenic nerve-diaphragm preparations isolated from mice (BALB/c strain) of both sexes of 20–25-g body weight. Animals were euthanized in accordance with the European Communities Council Directive (November 24, 1986; 86/609/EEC). The preparations were pinned to the bottom of a 3.5-ml translucent chamber and superfused with the following low Ca^{2+}, high Mg^{2+} Ringer's solution: 120.0 mM NaCl, 5.0 mM KCl, 0.5 mM $CaCl_2$, 11.0 mM $NaHCO_3$, 1.0 mM $NaHPO_4$, 5.0 mM $MgCl_2$, 11.0 mM glucose, pH 7.3–7.4. The solution flowed through the chamber at a rate of about 5 ml/min under continuous bubbling with 95% O_2 and 5% CO_2. Where indicated, 20 μM FCF was added into the perfusion solution that flowed through the chamber 1 h prior to the measurements of evoked and spontaneous secretion. This concentration of the inhibitor was chosen in preliminary experiments as the minimal concentration that altered spontaneous secretion. Exposure of nerve-diaphragm preparations to 100 μM FCF for more than 1 h resulted in a complete blockade of synaptic neurosecretion (not shown).

Suprathreshold stimuli of 0.1-ms duration were applied to the phrenic nerve with 0.5-Hz frequency via a suction electrode filled with the extracellular Ringer's solution. Nerve action potentials and evoked extracellular endplate currents (EPCs) were recorded using heat-polished, Ringer's solution-filled extracellular pipettes with tip diameters of 2–3 μm and a resistance of 1–3 megaohms. The extracellular pipette was positioned under visual control (magnification, 256×) near the nerve ending at a site where a three-phase nerve action potential could be recorded (40). The recorded signals were filtered between 0.03 and 10 kHz and digitized at 3-μs intervals by a nine-bit analog-digital converter, and the amplitude, rise time (between 20 and 80% of maximum amplitude), and time constants (τ) of the exponential decay of the EPC were calculated as described previously (41). To assess the level of spontaneous secretion, 100–150 spontaneous miniature EPCs were recorded without nerve stimulation, and their mean frequency was calculated. To control for the stability of the recording electrode next to the membrane region of interest during prolonged extracellular recording, only the data sets in which the amplitude of the nerve terminal action potentials as well as the rise and decay of miniature EPCs that varied less than 10% during the experiment were selected for further analysis.

The synaptic delay of evoked EPCs was measured as the time interval between the peak of the inward presynaptic Na^+ current and the time at which the rising phase of the EPC reached 20% of maximum (41, 42). The limit of the synaptic delay measurement was set at 50 ms. The EPCs after 1,000 nerve stimuli were collected to build the synaptic delay histograms (for details, see Refs. 41 and 43). The descending portions of the histograms were fitted to the double exponential function with a fast initial decay phase followed by a slower component. The decay of the first phase that ends at about 3 ms corresponds to the fast synchronous process of neurotransmitter release in response to the action potential. The second phase corresponds to the delayed asynchronous release of the neurotransmitter that persists longer than 3 ms after the nerve stimulation. To quantify the two components of the neurotransmitter release, the EPC signals within the time range of ≤3 ms were counted to quantify the synchronous release, and signals in the range of 3–50 ms were counted to quantify the delayed asynchronous release.

Determination of Basal and Influenza Virus-stimulated IL-6 Release by A549 Cells—A549 cells were seeded at 200,000 cells/well 24 h before the infection. All cells were seeded in 6-well plates and washed twice with DMEM without serum before the infection with influenza virus. Influenza virus A/WSN/33 (H1N1) was provided by Robert Lamb, Ph.D., Sc.D., Northwestern University, Evanston, IL. Cells were infected with 1 multiplicity of infection influenza virus, and after 8 h in the presence of the virus, they were treated with different concentrations of FCF for 16 h. At the end of the incubation, the culture medium was collected, and after washing with PBS, cells were lysed in lysis buffer (Cell Signaling Technology, Inc.). The amount of IL-6 in the medium was determined using an ELISA kit (Invitrogen) according to the manufacturer's instructions. The amount of septin-2, septin-7, retinoic acid-inducible gene-I, and β-actin in cell lysates was analyzed by Western blot.

Statistical Analysis—Statistical analysis was performed using Student's t test (GraphPad Prism 4 software and Microsoft Excel). Statistical significance and the number of experiments are specified in the figure legends.

RESULTS

Identification of Septin-interacting Proteins in Mouse Brain and Mammalian Cell Lines—To explore the mechanism of the involvement of septins in exocytosis, we analyzed the proteins co-immunoprecipitated with one of the major components of septin filaments, septin-2, from mouse brain extracts by nLC-MS/MS. The analysis identified nine other septins as major septin-2 interactors (Table 1), which is in agreement with numerous reports on the formation of hetero-oligomers between septin-2 and other septins (8) and makes it impossible to discern at this point whether other identified proteins interact directly with septin-2, other septins, or both. The list of septin interactors includes tubulins, actin, tubulin- and actin-binding proteins, several transmembrane proteins, signaling molecules, calcium-binding proteins, ubiquitin ligases, and deubiquitinating enzymes (data not shown) in agreement with

TABLE 1

Proteins immunoprecipitated by anti-septin-2 antibody from mouse brain extracts as detected by nLC-MS/MS analysis

sign., significant; seq., sequences; emPAI, exponentially modified protein abundance index.

Gene ID	Score	No. of matches	No. of sign. matches	No. of seq.	No. of sign. seq.	emPAI	Short description
Septins							
Sept2	1714	129	69	23	17	13.41	Septin-2
Sept7	1747	178	97	29	19	7.42	Septin-7
Sept11	1390	155	85	33	21	7.24	Septin-11
Sept8	1276	162	71	32	17	5.43	Septin-8
Sept6	670	106	39	23	10	1.96	Septin-6
Sept10	442	68	35	16	6	0.62	Septin-10
Sept9	284	63	22	32	10	0.73	Septin-9
Sept5	178	76	19	22	9	1.42	Septin-5
Sept3	116	32	12	14	7	1.03	Neuron-specific septin-3
Sept4	113	48	10	16	5	0.41	Septin-4
Vesicular trafficking/fusion/recycling							
Group A: neuronal							
Stxbp1	283	27	9	20	7	0.45	Syntaxin-binding protein1 (Munc-18-1)
Synj1	248	63	15	37	14	0.36	Synaptojanin-1
Syn2	117	29	4	13	4	0.22	Synapsin-2
Vapb	82	7	2	6	2	0.26	Vesicle-associated membrane protein-associated protein B
Syngr3	54	4	3	4	3	0.46	Synaptogyrin-3
Syp	34	12	1	4	1	0.1	Synaptophysin
Syt1	31	14	1	10	1	0.07	Synaptotagmin-1
Group B: ubiquitous							
Cltc	1385	131	72	66	42	1.51	Clathrin heavy chain
Flot1	1172	69	39	30	18	3.65	Flotillin-1
Flot2	696	67	29	24	14	2.14	Flotillin-2
Nsf	610	61	28	37	19	1.34	Vesicle-fusing ATPase
Arf1	327	30	11	12	5	1.46	ADP-ribosylation factor 1
Dnm1	175	38	11	27	9	0.35	Isoform 3 of Dynamin-1
Ap2a2	112	18	7	15	6	0.2	AP-2 complex subunit α-2
Ap3b2	90	35	2	23	2	0.06	AP-3 complex subunit β-2
Ap2s1	72	6	3	3	2	0.71	AP-2 complex subunit σ
Chaperones							
Sncb	2575	207	116	14	10	223.54	β-Synuclein
Hspa8	1846	161	85	38	26	8.57	Heat shock cognate 71-kDa protein (Hsc70)
Snca	894	131	57	13	10	84.55	α-Synuclein
Hspa5	549	64	27	30	16	1.32	78-kDa glucose-regulated protein
Hspa2	463	67	23	23	8	0.99	Heat shock 70-kDa protein 2
Hspa1b	361	42	16	17	7	0.65	Heat shock 70-kDa protein 1B

known roles of septins in organizing cortical cytoskeleton (10), clustering of plasma membrane proteins (7, 9), signaling pathways (21), calcium homeostasis (44), and degradation processes (8). A large group of septin interactors detected by nLC-MS/MS contained proteins involved in vesicle trafficking, vesicle/membrane fusion, or vesicle recycling (Table 1), which is the main focus of this study. Several proteins in this group, such as syntaxin-binding protein 1 (Munc-18-1), synaptojanin-1, and synapsin-2, are associated specifically with synaptic neurotransmission, whereas other proteins, such as clathrin, flotillins, and NSF, are known to be involved in endocytosis and intra-Golgi and endosomal vesicular transport in all eukaryotic cells. Another group of septin interactors includes molecular chaperones (Table 1), and some of these chaperones are known to be critical for exocytosis (1, 5, 6). All of the proteins listed in Table 1, except for other septins, have not been previously reported to interact with septin-2.

Western blot analysis of the proteins co-immunoprecipitated with septin-2 detected the interaction of septin-2 with β-synuclein, septin-7, and NSF (Fig. 1*A*) and Hsc70 (Fig. 1*B*) in the mouse brain. Syntaxin-1 was also detected in the septin-2 immunoprecipitates by Western blot analysis (Fig. 1*A*) in agreement with previously published results (19, 20). The interaction of septin-2 with NSF was also demonstrated in several mammalian cell lines (Fig. 1*C*). However, in the mouse brain as well as in cell lines, no interaction was detected between septin-2 and α-SNAP, the adaptor protein that mediates NSF binding to the SNARE complex (Table 1 and Fig. 1, *A* and *C*), indicating that septin interacts with free NSF but not with the NSF bound to the SNARE complex.

Quantification of Exocytosis by a Protein Secretion Assay in HEK-293 Cells—To study exocytosis, we established a protein secretion assay in HEK-293 cells by transfecting the cells with a vector encoding sec-β1, a soluble protein that corresponds to the extracellular domain of the dog Na,K-ATPase β_1 subunit. This protein has two features that make it useful to study protein secretion. First, when expressed in HEK-293 cells, it is rapidly accumulated in the culture medium (38), allowing fast and sensitive detection of protein secretion. Second, this secreted protein is *N*-glycosylated. Because *N*-glycans are covalently added to proteins co-translationally in the ER lumen and then undergo multiple modifications in consecutive compartments of the Golgi, analysis of the sec-β1 *N*-glycosylation state allows assessment of its vesicular trafficking through intracellular membrane compartments prior to its release into the medium, and it will allow us to discern specific intracellular trafficking events affected by septins.

Sec-β1 was efficiently secreted by constitutive exocytosis as a 40–45-kDa protein that was progressively accumulated in the culture medium for at least 5 h (Fig. 2*A*). In cell lysates, sec-β1 was detected as a major band at 35 kDa and a minor band at 40–45 kDa (Fig. 2*A*). These results demonstrate that cells contain both immature and mature forms of sec-β1, but only the mature form is secreted. Deglycosylation of both intracellular and extracellular forms of sec-β1 with peptide *N*-glycosidase F produced proteins of the same electrophoretic mobility corre-

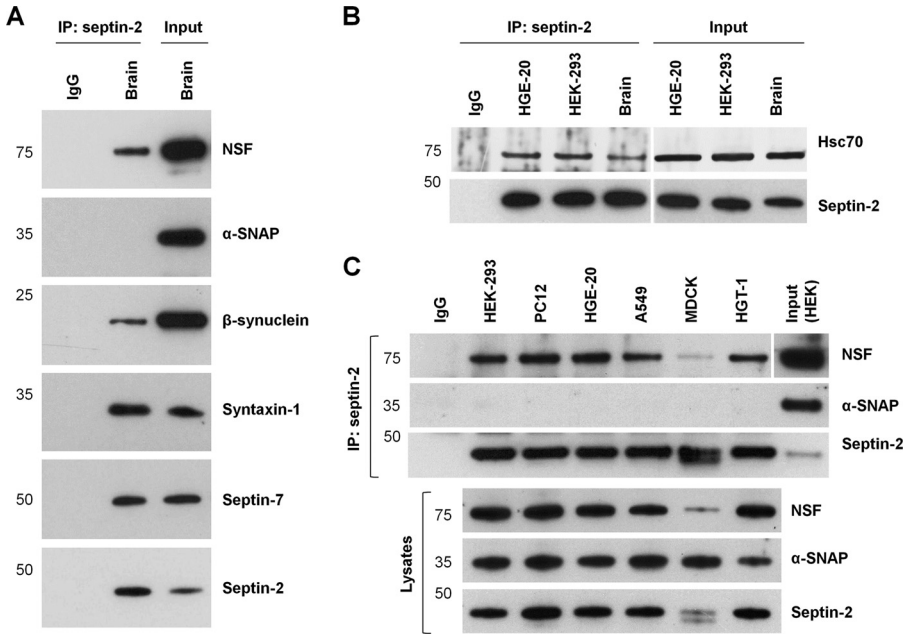

FIGURE 1. **NSF, β-synuclein, and Hsc70, but not α-SNAP, co-immunoprecipitate with septin-2.** *A*, NSF, β-synuclein, syntaxin-1, and septin-7, but not α-SNAP, were co-immunoprecipitated with septin-2 in mouse brain as detected by Western blot analysis. *B*, co-immunoprecipitation of Hsc70 with septin-2 was detected in mouse brain extracts and several cell lines. *C*, NSF, but not α-SNAP, was co-immunoprecipitated with septin-2 in various cell lines. 10% of the material used for immunoprecipitation (*IP*) was loaded in *Input lanes*.

sponding to the expected molecular mass of the core sec-β1 protein, 28 kDa (Fig. 2*B*, *lanes 5* and *6*). Endoglycosidase H (EndoH), which is known to cleave the high mannose and hybrid, but not complex-type, *N*-glycans, had no effect on the secreted fraction of sec-β1, indicating that all *N*-glycans in the mature exported sec-β1 are complex-type (Fig. 2*B*, *lane 3* and *steps 3* and *4* in the scheme). In contrast, only a minor fraction of the intracellular sec-β1 at 40–45 kDa was resistant to EndoH (Fig. 2*B*, *lane 4*). The major fraction of the intracellular sec-β1 was transformed by EndoH into the deglycosylated form of sec-β1, indicating that a significant fraction of sec-β1 present in cell lysates lacks any complex-type *N*-glycans and hence represents the newly synthesized molecules that have not yet exited from the ER (Fig. 2*B*, *lane 4* and *step 1*). The partially deglycosylated protein at 30–32 kDa seen in the EndoH-treated lysates is a product of the immature sec-β1 that has started to undergo the transformation of its *N*-glycans in the Golgi and hence has both EndoH-sensitive and EndoH-resistant *N*-glycans (Fig. 2*B*, *lane 4* and *step 2*). Therefore, cell lysates contain mostly the immature forms of sec-β1 and only a small amount of the mature sec-β1, demonstrating that the newly synthesized sec-β1 is secreted to the medium as soon as it traffics through the Golgi and trans-Golgi network.

Septins Are Important for Constitutive Protein Secretion—HEK-293 cells were transfected with septin-2-specific siRNA twice, 72 and 24 h prior to the experiment, as described under "Experimental Procedures." This two-step transfection decreased the septin-2 level by 70% and decreased the septin-7 level by 62% (Fig. 3*A*). However, a one-step transfection with septin-2 siRNA followed by 24-h cell incubation decreased the level of septin-2 by 66% but did not alter the level of septin-7 (see Fig. 6*B*). The reduction in septin-7 by a prolonged presence of septin-2 siRNA in cells was not likely a result of off-target effects of siRNA because the two regions selected for siRNA duplexes were specific to the septin-2 sequence and not homologous to septin-7 or other known proteins. A decrease in septin-7 level presumably occurs due to post-translational down-regulation. It is known that septins exhibit a coordinated regulation of their levels. Particularly, knockdown of septin-7 decreased the level of septin-2 (45–47). The level of expression of septin-9 was not affected by a two-step (not shown) or one-step transfection with septin-2 siRNA (see Fig. 6*B*). Septin-2 silencing slightly altered the intracellular distribution of septin-9 by increasing the size of septin-9-containing filaments (Fig. 4*B*).

A two-step transfection with septin-2 siRNA reduced the accumulation of sec-β1 in the medium by 32%, did not change the amount of the immature form of sec-β1, and increased the amount of its mature form by 18% in cell lysates (Fig. 3*B*). Similar changes in cell lysates and medium were observed after a 24-h exposure to septin-2 siRNA (data not shown). Protein secretion was also reduced by depleting one of the important components of the exocytosis machinery, NSF. Transfection of cells with NSF-specific siRNA resulted in a decrease in the cellular amount of NSF by 90% (Fig. 3*A*), decreased the amount of sec-β1 secreted into the medium by 20%, and increased the amount of the mature sec-β1 inside cells by 12% as compared with the cells transfected with the control siRNA (Fig. 3*B*). However, silencing of α-SNAP, which in addition to mediating NSF binding to SNARE complexes is known to be involved in the ER to Golgi trafficking (48), affected protein secretion differently. Transfection of HEK-293 cells with α-SNAP-specific siRNA decreased the level of α-SNAP by 85% (Fig. 3*A*), almost completely prevented sec-β1 accumulation in the medium, increased accumulation of the immature form of sec-β1, and

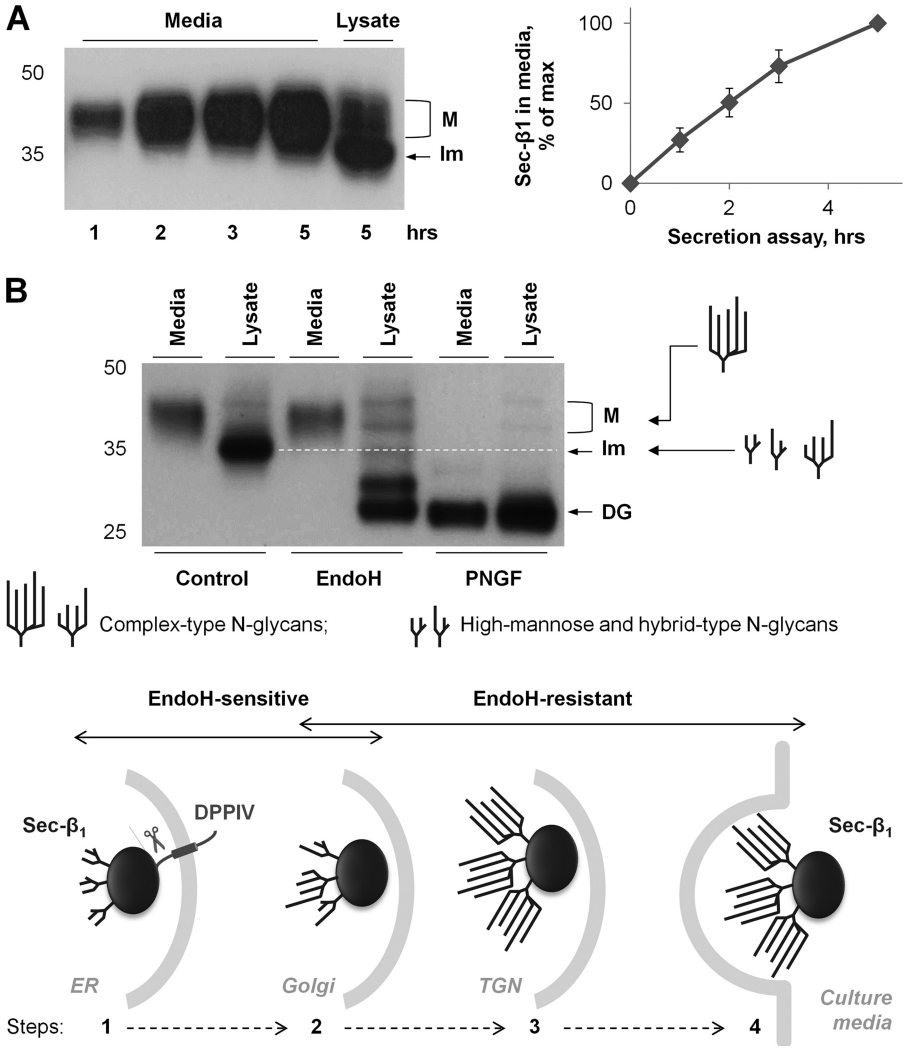

FIGURE 2. **Protein secretion assay in HEK-293 cells.** *A*, sec-β1 accumulated in the medium during 5-h cell incubation of HEK-293 cells transiently transfected with Sec-β1 plasmid as detected by Western blot analysis. The secreted form of sec-β1 has lower electrophoretic mobility as compared with that of the intracellular form. Densitometry quantification of the results of three experiments shows almost linear accumulation of sec-β1 in the medium. *B*, analysis of *N*-glycans of sec-β1 present in the medium and cell lysates using EndoH and peptide *N*-glycosidase F (*PNGF*) showed that all secreted molecules have exclusively mature EndoH-resistant complex-type *N*-glycans. By contrast, only a minor fraction of intracellular molecules have EndoH-resistant complex-type *N*-glycans. The scheme below the blot shows that sec-β1 is synthesized as a precursor containing a transmembrane domain of DPPIV fused to the N-terminal end of the extracellular domain of the Na,K-ATPase β_1 subunit. During translation of the DPPIV-sec-β1 chimera, the hydrophobic sequence of the DPPIV transmembrane domain is inserted in the ER membrane, resulting in the translocation of sec-β1 to the ER lumen followed by a covalent addition of *N*-glycans to sec-β1. Because of the presence of the engineered ER signal peptidase cleavage site between DPPIV and sec-β1 (38), sec-β1 is released into the ER lumen, traffics through the Golgi where its *N*-glycans are transformed to EndoH-resistant complex-type chains by the Golgi glycosyltransferases, and is secreted to the medium. Only the mature sec-β1 that has all complex-type, EndoH-resistant *N*-glycans is secreted. *M*, mature form of sec-β1; *Im*, immature form of sec-β1; *DG*, deglycosylated form of sec-β1; *TGN*, trans-Golgi network.

resulted in the disappearance of the mature form of sec-β1 in cell lysates (Fig. 3*B*).

Cell exposure to 100 μM FCF, which has been previously shown to impair septin dynamics in yeast and mammalian cells (27–29), significantly altered the intracellular distribution of both septin-2 and septin-9 by increasing the size of their filaments (Fig. 4). The addition of 100 μM FCF to HEK-293 cells decreased the amount of sec-β1 released to the medium during a 1-h secretion assay by 63% and almost completely blocked secretion in cells preincubated with the inhibitor for 1 h (Fig. 5). Exposure of cells to 50 and 25 μM FCF for 1 h inhibited exocytosis by 56 and 40%, respectively (data not shown). The glycosylation pattern and the amount of the immature sec-β1 in cell lysates did not change, whereas the amount of mature sec-β1 was increased in cells exposed to FCF (Fig. 5). By contrast, the inhibitor of microtubule polymerization, nocodazole, dramatically decreased the amount of mature sec-β1 both in the medium and cell lysate (Fig. 5).

Accumulation of sec-β1 in the medium was reduced by a one-step transfection of septin-2 siRNA and cell exposure to FCF in the presence of cycloheximide (Fig. 6, *A* and *C*). To evaluate the effects of septin-2 siRNA and FCF on the rates of intracellular trafficking of the newly synthesized sec-β1, we studied the time course of alterations in the levels of its immature and mature forms in cell lysates in the absence of protein synthesis. The decrease in the amount of the immature ER-resident form of sec-β1 in control cells (Fig. 6, *A* and *D*) is a result of its trafficking from the ER to the Golgi where it undergoes

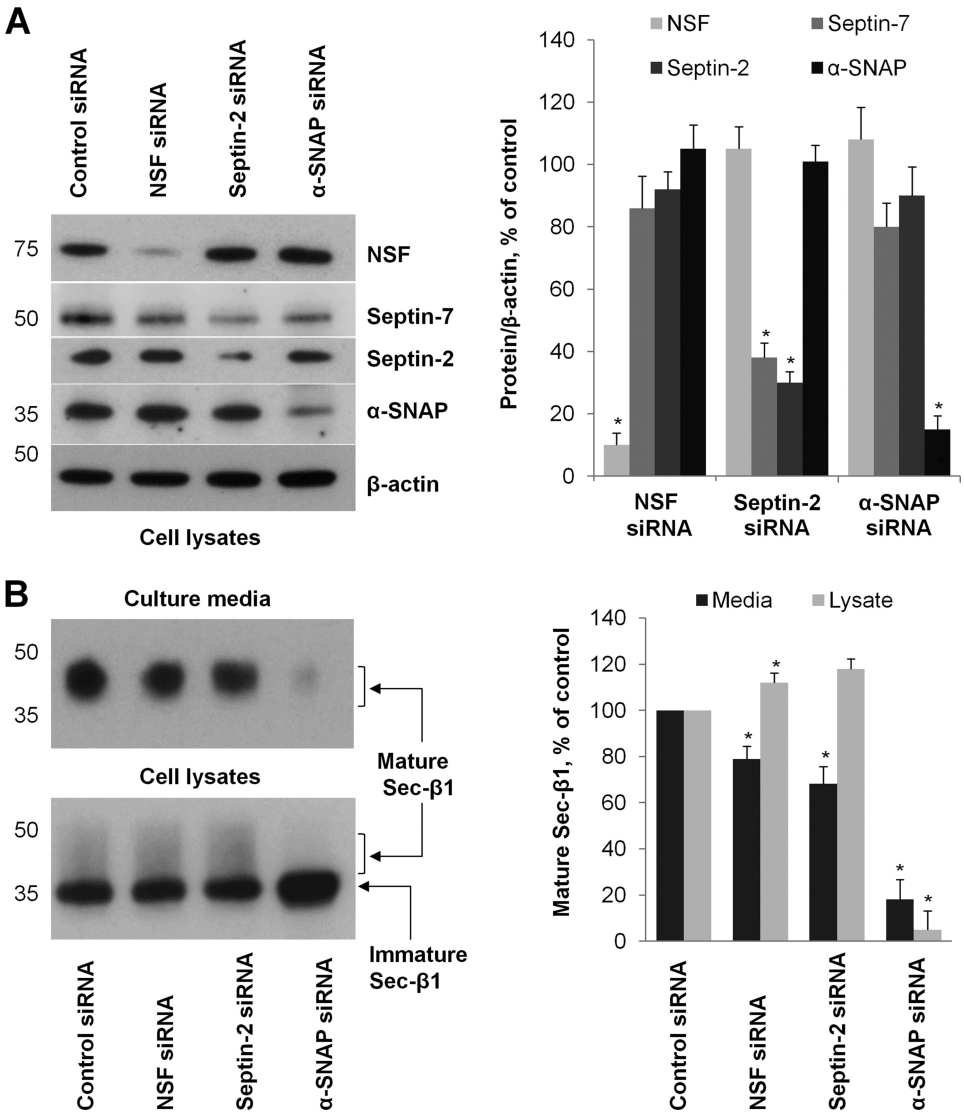

FIGURE 3. **Protein secretion is inhibited by knockdown of septin-2.** *A*, a two-step transfection of cells with specific siRNAs resulted in knockdown of the respective proteins. Septin-2 siRNA resulted in a decrease in levels of septin-2 itself and of septin-7. *B*, knockdown of septin-2/septin-7 or NSF decreased accumulation of mature sec-β1 in the culture medium as detected by a 1-h secretion assay and increased the amount of the mature sec-β1 in cells. Knockdown of α-SNAP almost completely eliminated the presence of the mature sec-β1 both in cells and in the medium and produced accumulation of the immature sec-β1 in cells. The amount of β-actin in cell lysates was determined on the same blots to confirm equal loading. Densitometric quantification was performed for three independent experiments. *Error bars*, S.D. ($n = 3$); *, significant difference from the control, $p < 0.01$, Student's *t* test.

maturation and acquires complex-type carbohydrate chains (Fig. 2*B*, *step 2*). The decline in the immature form was not altered by septin-2 siRNA or the exposure of cells to FCF (Fig. 6, *A* and *D*), indicating no effect of these treatments on the ER to Golgi trafficking of sec-β1 carriers. The decrease in the amount of the mature sec-β1 in control cells (Fig. 6, *A* and *E*) indicates that, in the absence of protein synthesis, the release of sec-β1 into the medium is more rapid than its trafficking from the ER to the Golgi. This decrease in the level of the mature form was partially abolished by septin-2 siRNA and almost completely prevented by FCF (Fig. 6, *A* and *E*), indicating that both septin silencing and FCF induce the intracellular accumulation of the post-Golgi forms of sec-β1.

Therefore, both silencing of septin-2 and cell exposure to FCF decrease constitutive secretion of a model protein and increase intracellular accumulation of the post-Golgi species of this protein but do not affect its delivery to and maturation in the Golgi. These effects are in contrast to those of α-SNAP depletion or cell exposure to nocodazole, which inhibits protein secretion by preventing trafficking from the ER to the Golgi.

Disruption of Normal Septin Organization and Dynamics by FCF Inhibits Influenza Virus-induced Cytokine Release by A549 Cells—To study whether septin-2 plays a role in stimulated secretion, we analyzed the secretion of cytokines, a hallmark of inflammatory response. We studied the effect of FCF on control and influenza virus-induced secretion of IL-6 by lung epithelial A549 cells. Alveolar epithelial cells are primary targets of influenza virus. Exposure to the virus increases secretion of IL-6 and other inflammatory cytokines that are the earliest antiviral responses in these cells (49). IL-6 is synthesized as a precursor containing a signal sequence that

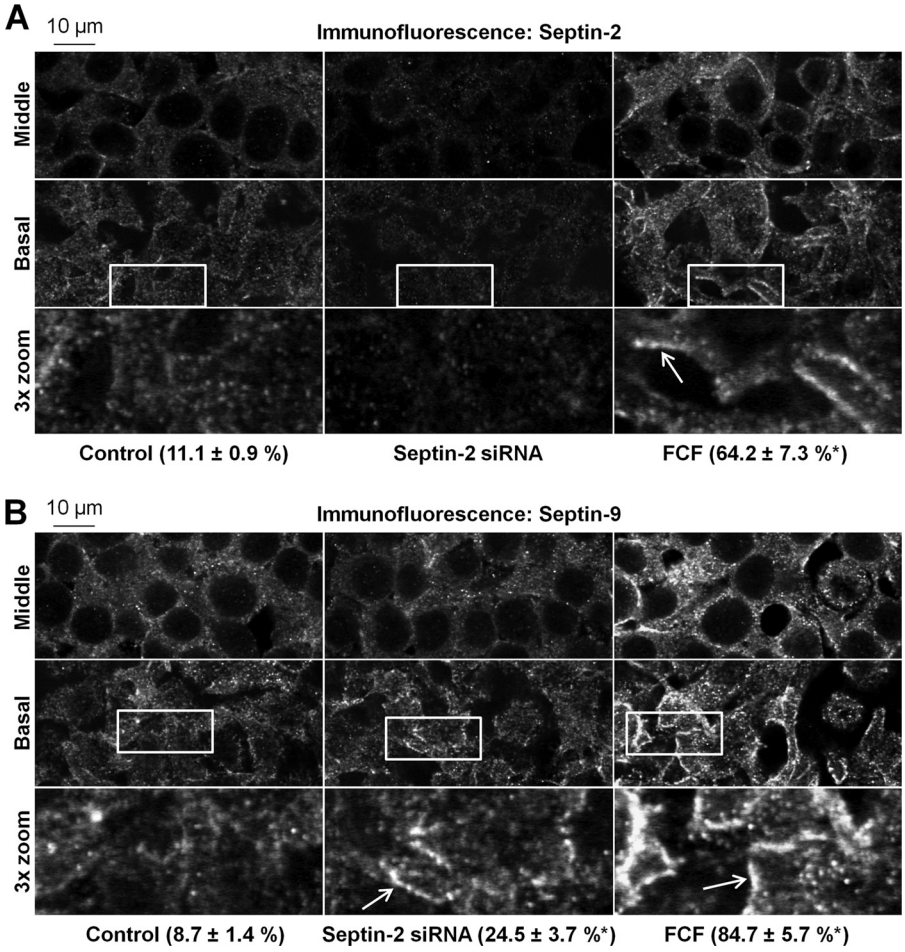

FIGURE 4. **Both transfection with septin-2 siRNA and exposure to FCF alter the intracellular distribution of septin-2 and septin-9 in HEK-293 cells.** A one-step transfection of cells with septin-2 siRNA decreased immunofluorescence of septin-2 (*A*) and altered the distribution of septin-9 (*B*). Cell exposure to 100 μM FCF for 3 h induced the formation of larger septin-2-containing (*A*) and septin-9-containing (*B*) structures. Enlarged images of the *boxed fields* are shown in the *bottom panels* in *A* and *B*. The percentage of cells containing continuous septin-2- or septin-9-positive structures that are longer than 2 μm (*arrows*) is shown below the images. Calculations were performed by analyzing at least 10 confocal microscopy images per condition for each of the three independent experiments. Each image contained at least 20 cells. The intensity of septin-2 immunofluorescence in siRNA-treated cells was too low to perform the calculations. *Scale bar*, 10 μm. *, significant difference from the control, $p < 0.05$, Student's *t* test.

allows the translocation of the protein into the ER lumen. After cleavage of a signal peptide, IL-6 traffics through the Golgi and recycling endosomes and is secreted by SNARE-mediated exocytosis (50).

Infection of A549 cells with influenza A/WSN/33 H1N1 virus induced the intracellular expression of retinoic acid-inducible gene-I protein, which acts as a sensor for the influenza virus RNA and leads to the release of proinflammatory cytokines (51). Infection of A549 cells with the virus increased the secretion of IL-6 by more than 10-fold (Fig. 7*A*). The increase in secretion correlated with the increase in mRNA levels for IL-6 (data not shown) as reported previously (49). Exposure of cells to 25 μM FCF for 16 h did not alter the virus-induced expression of retinoic acid-inducible gene-I but significantly inhibited secretion of IL-6 (Fig. 7, *A* and *B*). The level of the intracellular IL-6 was not decreased, showing that FCF did not inhibit transcription or translation of IL-6. Exposure of cells to 25 μM FCF did not alter the level of endogenous septin-2 and septin-7 (Fig. 7*B*) but resulted in their reorganization as evidenced by the increased size of septin-2 filaments (Fig. 7*C*). Similar results were observed in the presence of 50 and 100 μM FCF (data not shown). Therefore, disruption of septin dynamics inhibits both basal and virus-stimulated cytokine release.

Septins Are Important for Exocytosis of Transmembrane Proteins—To determine whether septins are also involved in the constitutive exocytosis of transmembrane proteins that leads to the insertion of these proteins in the plasma membrane, we used stable cell lines expressing a YFP-tagged Na,K-ATPase β_1 subunit, a GFP-tagged Na,K-ATPase α_1 subunit, or YFP-tagged basolateral bile acid transporter. All three fusion proteins reside almost exclusively in the plasmalemma in control cells (Fig. 8, *A–C*). Transfection with septin-2 siRNA increased intracellular vesicular accumulation of the Na,K-ATPase β_1 subunit in HEK-293 (Fig. 8*A*) and Na,K-ATPase α_1 subunit in A549 cells (Fig. 8*B*). Cell exposure to 100 μM FCF for 3 h resulted in similar intracellular vesicular accumulation of the Na,K-ATPase β_1 subunit in HEK-293 cells (not shown), Na,K-ATPase α_1 subunit in A549 cells (Fig. 8*B*), or bile acid transporter in MDCK cells (Fig. 8*C*). Exposure to FCF altered the distribution and size of septin-2 filaments in MDCK cells (Fig. 8*D*). The vesicular accumulation of the transmembrane

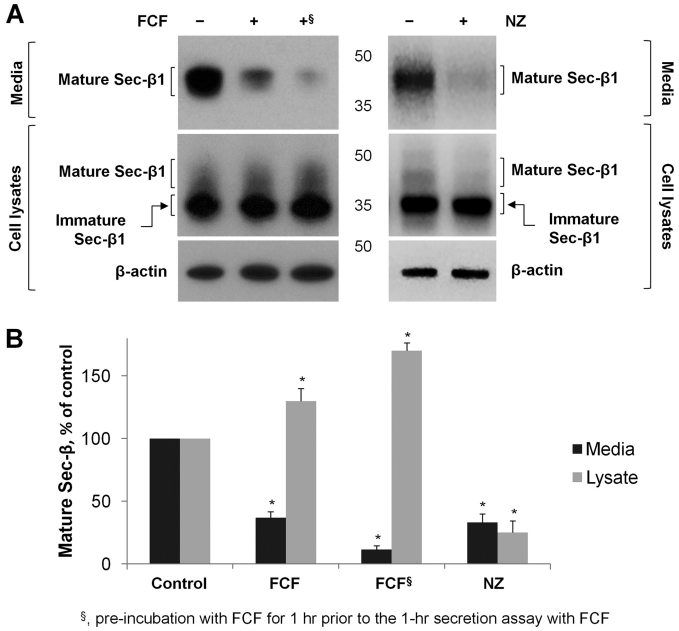

FIGURE 5. **The impairment of septin dynamics by FCF inhibits protein secretion in HEK-293 cells.** *A*, the amount of sec-β1 released to the medium during a 1-h secretion assay in the absence or presence of 100 μM FCF or 0.5 μM nocodazole (*NZ*) was determined by immunoblotting in parallel with the analysis of the intracellular fractions of sec-β1. Where indicated, cells were preincubated with 100 μM FCF prior to the addition of fresh medium and starting the secretion assay. The amount of β-actin in cell lysates was determined on the same blots to confirm equal loading. *B*, densitometric quantification performed for three independent experiments showed that both inhibitors significantly reduced secretion but differently affected the levels of intracellular fractions of sec-β1. *Error bars*, S.D. ($n = 3$); *, significant difference from the control, $p < 0.01$, Student's *t* test.

proteins in septin-depleted or FCF-exposed cells contrasts with predominant ER retention of the Na,K-ATPase β_1 subunit in α-SNAP-depleted HEK-293 (Fig. 8*A*). The results clearly indicate that transfection of cells with septin-2 siRNA or cell exposure to FCF does not impair the ER to Golgi trafficking of the transmembrane proteins. Also, these results suggest that septin depletion or FCF attenuates insertion of transmembrane proteins into the plasma membrane.

To confirm or rule out the latter hypothesis, we determined the effect of FCF on the rate of exocytosis of transmembrane proteins by using a stable cell line expressing the YFP-tagged basolateral bile acid transporter. In confluent MDCK cells, this protein is localized almost exclusively to the lateral membrane as is evident in the horizontal and vertical confocal microscopy sections of the cell monolayer (Fig. 8*C*). By incubating confluent cells in Ca^{2+}-free PBS for 60 min, we disrupted intercellular junctions, but cells remained attached to the surface (Fig. 9*A*, *left panels*). Such treatment is known to result in the endocytosis of the proteins located at the lateral membrane. Accordingly, Ca^{2+} depletion resulted in full internalization of the bile acid transporter in 40% of cells and partial internalization of the transporter in the rest of cells (Fig. 9, *A* and *B*). Replacement of PBS with a Ca^{2+}-containing culture medium with or without FCF resulted in exocytosis and reinsertion of the transporter in the plasmalemma, which we monitored by time lapse confocal microscopy. In the absence of FCF, the internalized transporter was detected in the plasmalemma in the majority of the cells after 7 min of cell incubation in the Ca^{2+}-containing medium and was found in the plasmalemma in all cells after 35 min (Fig. 9, *A*, *arrows*, and *B*). In the presence of FCF, reinsertion occurred more slowly, and the transporter was not seen at the surface in 20% of cells even after 35 min (Fig. 9, *A*, *arrowheads*, and *B*). The intercellular junctions were re-established between all cells 2 h after adding back Ca^{2+} both in the absence and in the presence of FCF (Fig. 9*C*). However, in the absence of FCF, the transporter was predominantly detected in the plasmalemma, whereas in the presence of FCF, the transporter was seen both in the plasmalemma and in intracellular vesicles (Fig. 9*C*). The results show that insertion of the transporter into the lateral membrane was significantly attenuated by FCF.

FCF Inhibits Both Spontaneous and Stimulated Neurotransmitter Release in Motor Neurons—To study the involvement of septins in exocytosis of neuronal synaptic vesicles, we measured neurotransmitter release in mouse phrenic nerve-diaphragm preparations using electrophysiological methods. The frequency of spontaneous miniature EPCs detected without nerve stimulation was decreased by 30% after a 60-min exposure to 20 μM FCF (Fig. 10*A*). The synchronous and delayed asynchronous phases of evoked secretion were inhibited in the presence of FCF by 21 and 50%, respectively (Fig. 10*B*). In addition, FCF altered the kinetics of secretion by altering the duration of a synaptic delay, which is the time interval between the arrival of an action potential at the nerve terminal and the initiation of the evoked EPCs. Incubation of nerve-diaphragm preparations with 20 μM FCF for 1 h decreased the number of EPCs with long synaptic delays (Fig. 10*C*), seen as a reduced "tail" in the distribution of synaptic delays (Fig. 10*D*). Hence, the cumulative curve was shifted toward smaller values of synaptic delays as compared with that in the control (Fig. 10*E*). Therefore, the impairment of septin assembly/disassembly inhibits both spontaneous and evoked neurotransmitter secretion.

Aberrant Assembly and Disassembly of Septin Oligomers Alter the Interactions between the Components of the Exocytosis Apparatus—Exposure of cultured undifferentiated neuroendocrine PC12 cells to 100 μM FCF for 2 h decreased the amount of Hsc70 co-immunoprecipitated with SNAP-25 by 21% (Fig. 11, *A* and *B*). 24-h incubation with FCF decreased the amount of SNAP-25-bound Hsc70 by 48% (Fig. 11, *A* and *B*). In parallel, 24-h incubation of cells with FCF reduced the total amount of SNAP-25 in cell lysates by 51% (Fig. 11, *A* and *B*). These results show that FCF impairs the interaction between SNAP-25 and its chaperone Hsc70 and hence increases the susceptibility of SNAP-25 to degradation.

In addition, FCF exposure decreased the resistance of SNARE complexes to dissociation by SDS. In PC12 cell lysates that were preincubated in SDS-containing buffer at 25 °C prior to SDS-PAGE, syntaxin-1 was detected by Western blotting as two bands (Fig. 11*C*). The lower band at 35 kDa corresponds to a monomeric form of syntaxin-1, whereas the upper wide band corresponds to partially disassembled SNARE complexes. The ratio between free and complex-bound syntaxin-1 was increased by FCF (Fig. 11, *C* and *D*), suggesting that impairment of septin dynamics by the inhibitor destabilizes the SNARE complexes. Boiling of samples resulted in complete dissociation

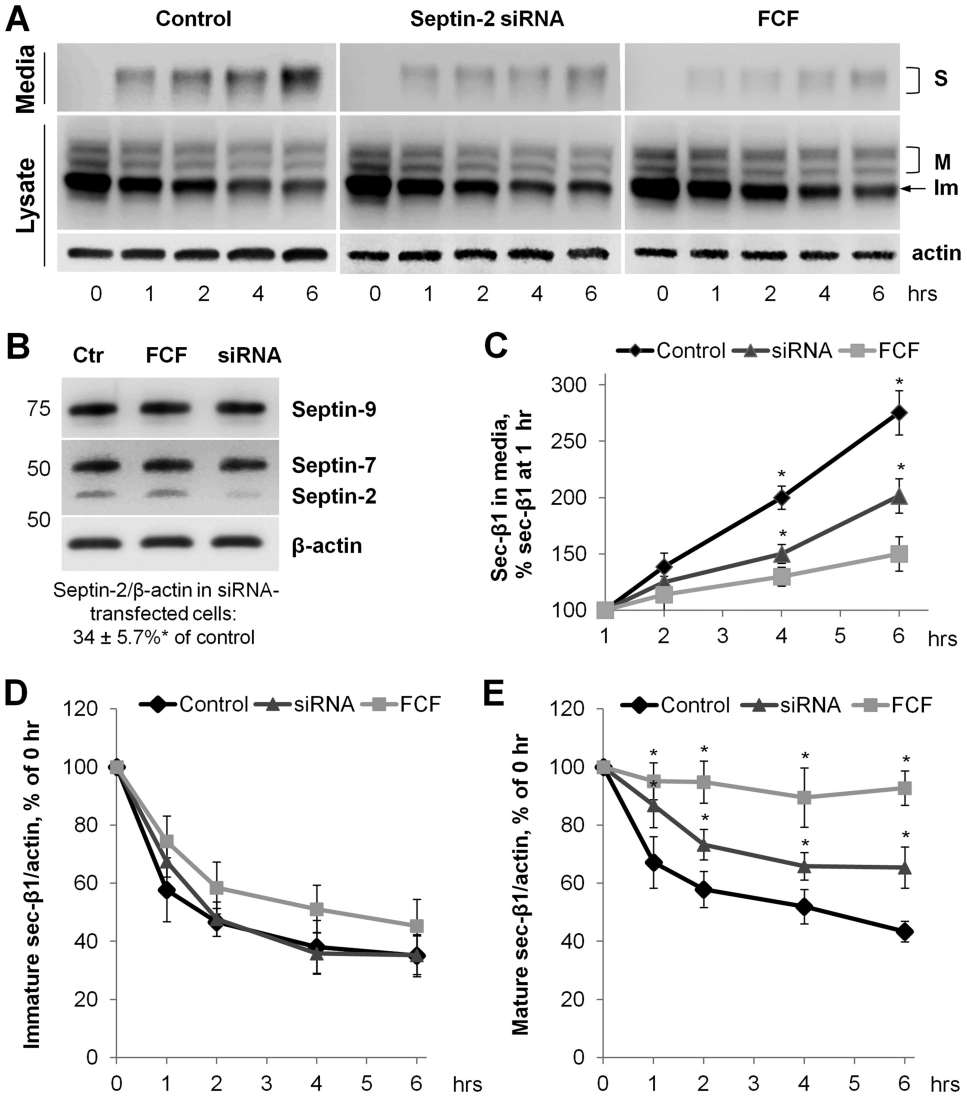

FIGURE 6. **Down-regulation of septin-2 or impairment of septin organization by FCF delays the release of Sec-β1 into medium but not the delivery of Sec-β1-carrying vesicles from the ER.** *A*, HEK-293 cells expressing sec-β1 were transfected with septin-2 or negative control siRNA as described under "Experimental Procedures." Cells were incubated for the indicated periods of time with 20 μg/ml cycloheximide with or without 100 μM FCF as indicated. The amount of sec-β1 in the medium and cell lysates was determined by immunoblotting. The amount of β-actin in cell lysates was determined on the same blots to account for variability in loading. *B*, exposure of HEK-293 cells to 100 μM FCF for 3 h did not alter the total amount of septin-2 or septin-7 as compared to control (*Ctr*). A one-step transfection of cells with septin-2 siRNA decreased the total level of septin-2 but not the levels of septin-7 or septin-9. *C–E*, densitometry quantification of the results of three parallel experiments showed that in control cells accumulation of the secreted (*S*) form of sec-β1 in medium was accompanied by a decrease in levels of both immature (*Im*) and mature (*M*) forms in lysates (*left panels*). Both septin-2 silencing and cell exposure to FCF reduced the rate of sec-β1 accumulation in the medium (*C*). The decline in the immature form was not affected by septin-2 siRNA (*D*). The level of the mature form was moderately attenuated by down-regulation of septin-2 by siRNA and almost completely prevented by cell exposure to FCF (*E*). *Error bars*, S.D. ($n = 3$ independent experiments); *, significant difference from the same time point in control, $p < 0.05$, Student's *t* test.

of SNARE complexes and detection of exclusively monomeric forms of syntaxin-1 (Fig. 11*C*). Only a monomeric form of NSF was detected in boiled and non-boiled lysates of PC-12 cells (Fig. 11*C*). Therefore, interference with septin oligomerization alters the interactions between the proteins of the membrane fusion machinery.

DISCUSSION

Septin-2 Stimulates Exocytosis—The results presented here demonstrate that the rate of constitutive protein secretion is reduced by partial depletion of septin-2 and septin-7 (Fig. 3) or septin-2 alone (Fig. 6, *B* and *C*), indicating that septin-2 facilitates protein secretion. These data contrast with previously published data on the inhibitory effect of septin-5 on protein secretion (20, 24). Protein secretion is a complex process that includes trafficking of the newly synthesized protein through the biosynthetic vesicular pathway followed by docking of mature secretory vesicles in the plasma membrane and the SNARE-mediated membrane fusion of these vesicles with the plasmalemma. The intracellular transport of vesicles both from the ER to the Golgi and from the Golgi to the plasma membrane is microtubule-dependent (52), and septins are known to regulate the stability and growth of microtubules (46, 47, 53–56). Thus, it is crucial to distinguish between the effects of septin silencing on the transport of vesicles from the ER to the plasma membrane and the effects of this treatment on the final stages of

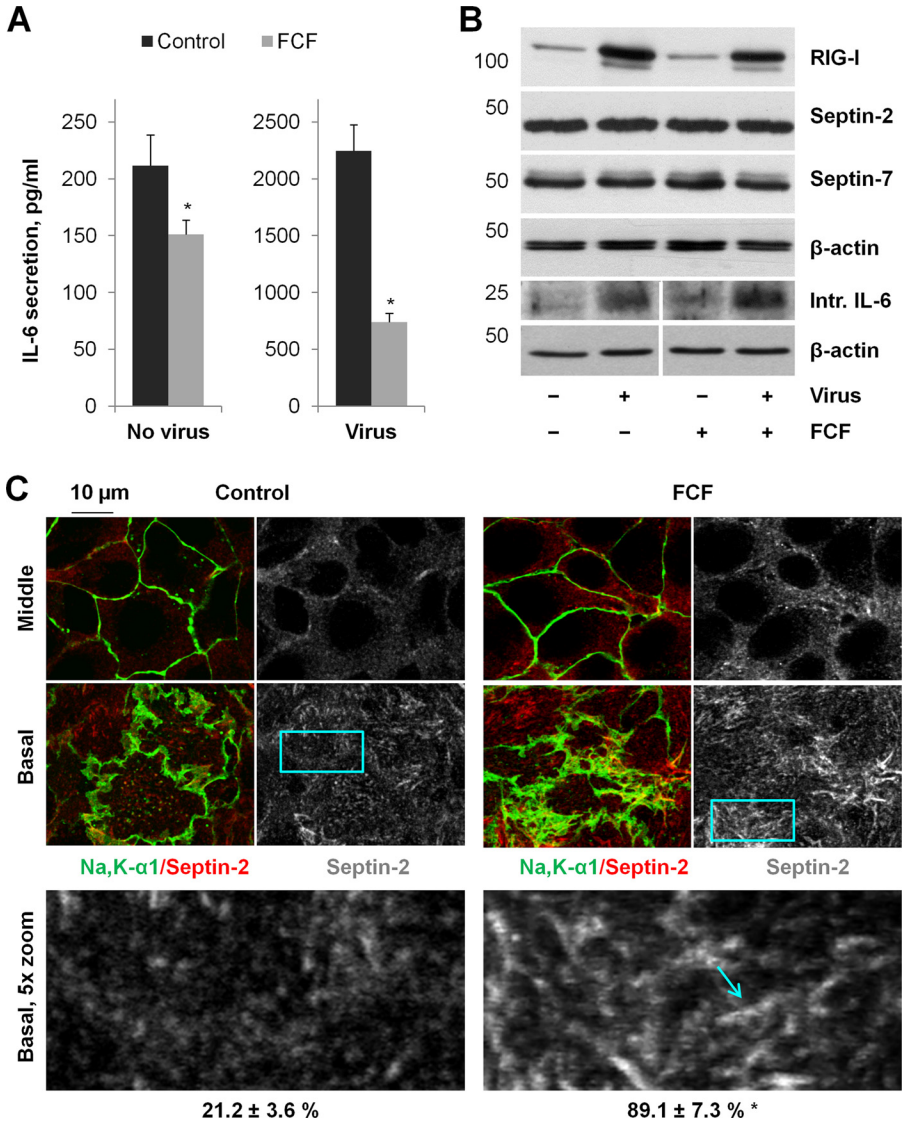

FIGURE 7. **The impairment of septin dynamics by FCF inhibits both basal and virus-induced cytokine secretion in lung epithelial cells.** *A*, FCF inhibited both basal and virus-induced cytokine IL-6 secretion by A549 cells. *B*, exposure to FCF did not alter the expression level of septin-2 and septin-7 or the virus-induced increase in the amount of a cytoplasmic sensor of viral nucleic acids, retinoic acid-inducible gene-I (*RIG-I*), and intracellular IL-6 (*Intr. IL-6*). *C*, exposure of lung epithelial A549 cells to 25 μM FCF for 16 h induced the formation of larger septin-2-containing aggregates as detected by septin-2 immunofluorescence (*red*) and altered the cell shape. The *green* fluorescence of the stably expressed GFP-tagged Na,K-ATPase α1 subunit shows the outlines of the cells. Enlarged images of *boxed fields* are shown in *bottom panels*. The percentage of cells containing continuous septin-2- or septin-9-positive structures that are longer than 2 μm (*arrow*) is shown below the images. Calculations were performed as described in the legend of Fig. 4. *Scale bar*, 10 μm. *Error bars*, S.D. (n = 3 independent experiments); *, significant difference from the control, $p < 0.01$, Student's t test.

exocytosis. Such a distinction has not been made in previous studies on the roles of septin-4 and septin-5 in exocytosis (16, 17, 24).

Here, we took advantage of a secretion assay in HEK-293 cells that allowed us to determine the localization of the secreted protein during its passage through the biosynthetic secretory pathway based on the glycosylation pattern of sec-β1 (Fig. 2). The experiments performed in the absence of protein synthesis demonstrated that both the septin-2 siRNA and cell exposure to FCF reduce the rate of protein secretion and induce the intracellular accumulation of the post-Golgi sec-β1 carriers but do not alter the rate of the ER to trans-Golgi network trafficking (Fig. 6). As a result, septin silencing or impairment of septin dynamics by FCF reduces the amount of secreted protein in the medium and increases the intracellular level of the mature protein under steady state conditions (Figs. 3 and 5). Therefore, the newly synthesized sec-β1 molecules traffic normally through the Golgi but, due to the impaired exocytosis, accumulate inside the cells. In addition, FCF decreases the rate of exocytosis of internalized transmembrane proteins, leading to their insertion into the plasmalemma (Fig. 9). Therefore, post-Golgi steps of exocytosis, rather than transport of vesicles from the ER to the Golgi, are impaired by septin-2 siRNA or FCF.

The inhibition of microtubule polymerization with nocodazole dramatically inhibited the ER to Golgi trafficking of sec-β1 (Fig. 5), consistent with previously published results on the acute inhibition of ER to Golgi trafficking by microtubule disruption (57). These results render the possibility that impairment of microtubules by septin-2 siRNA or FCF attenuates the vesicle transport from the Golgi to the plasma membrane but has no effect on vesicle transport from the ER to the Golgi

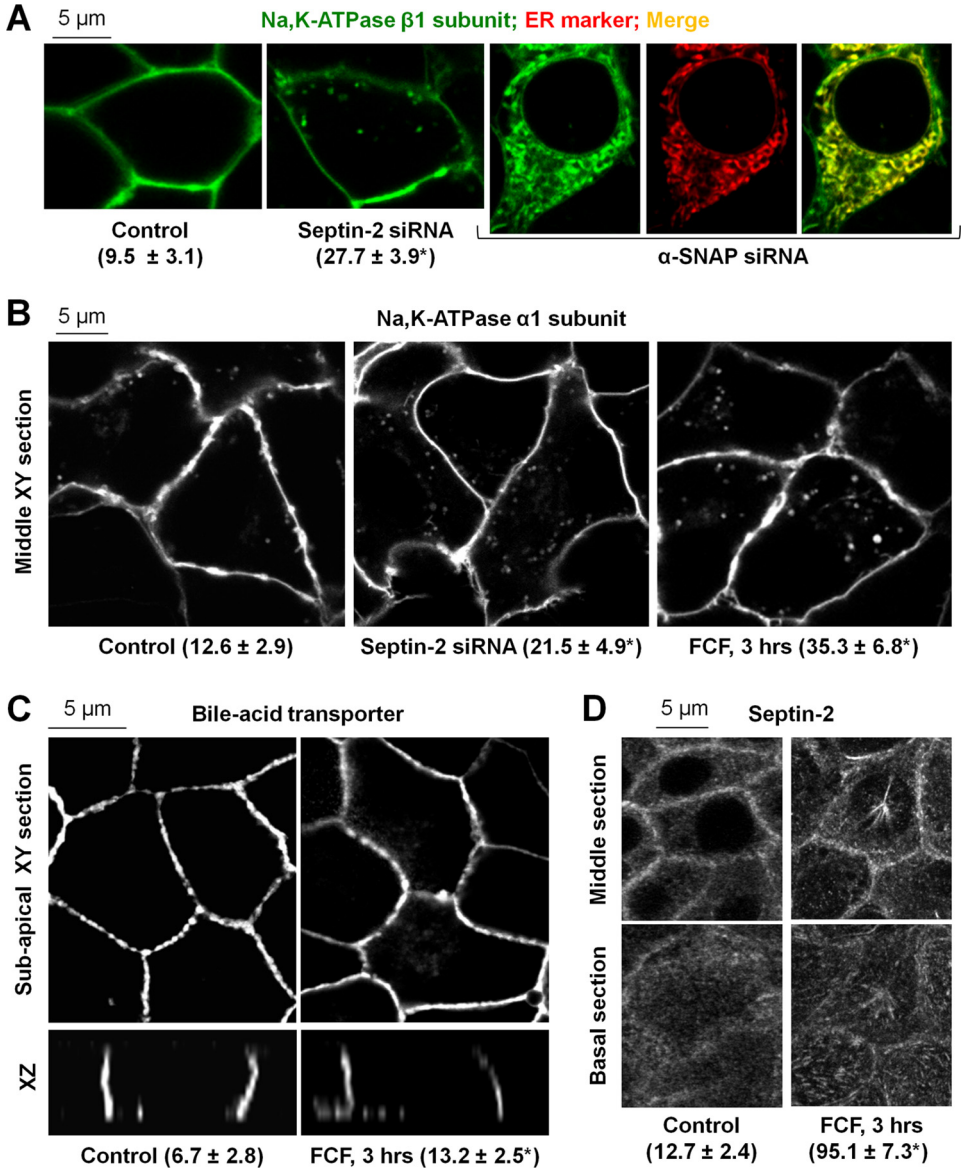

FIGURE 8. **Down-regulation of septin-2 or impairment of septin organization by FCF increases intracellular accumulation of integral transmembrane proteins in various cells.** *A*, confocal microscopy images of HEK-293 cells stably expressing the YFP-linked Na,K-ATPase β_1 subunit (*green*) show that transient transfection of cells with septin-2 siRNA resulted in accumulation of the Na,K-ATPase β_1 subunit-containing intracellular vesicles. By contrast, transient transfection of these cells with α-SNAP siRNA resulted in major accumulation of the Na,K-ATPase β_1 subunit in the ER as demonstrated by co-localization with a fluorescent ER marker (*red*). *B* and *C*, transfection of A549 cells stably expressing GFP-tagged Na,K-ATPase α_1 subunit with septin-2 siRNA or cell exposure to 100 μM FCF (*B*) or incubation of MDCK cells stably expressing YFP-tagged basolateral bile acid transporter with 100 μM FCF (*C*) resulted in accumulation of cargo-containing intracellular vesicles. The ratio between the intracellular fluorescence intensity and the total cellular fluorescence intensity is shown below the images on *A–C*. Calculations were performed by analyzing at least 10 confocal microscopy images per condition for each of the three independent experiments. At least five cells were analyzed in each image. *D*, exposure of MDCK cells to 100 μM FCF for 3 h induced the formation of larger septin-2-containing aggregates as detected by septin-2 immunofluorescence. The percentage of cells containing continuous septin-2- or septin-9-positive structures that are longer than 2 μm is shown below the images. Calculations were performed as described in the legend of Fig. 4. *Scale bar*, 5 μm. *, significant difference from the control, $p < 0.05$, Student's *t* test.

extremely unlikely. Therefore, the presence of septin-2 and its continuous assembly and disassembly with other septins are important for the late steps of exocytosis, such as vesicle docking to or vesicle fusion with the plasmalemma.

In support of this conclusion, the alterations in the amount of secreted and intracellular sec-β1 by septin-2 siRNA were strikingly similar to those caused by silencing of NSF (Fig. 3), which is known to be essential for exocytosis (1, 2). In addition, the impairment of septin dynamics acutely inhibited the rate of acetylcholine release in mouse motor neurons (Fig. 10), which depends on the pool of fusion-competent neurotransmitter-loaded synaptic vesicles rather than the microtubule-dependent delivery of new vesicles from the ER and Golgi (58). All three known modes of neurotransmitter release, spontaneous, synchronous, and asynchronous, were inhibited (Fig. 10). Spontaneous neurotransmitter release occurs in the absence of nerve stimuli, synchronous release occurs within several milliseconds after action potential generation in a presynaptic membrane, and asynchronous release persists longer after an action potential (59, 60). At the molecular level, these three modes

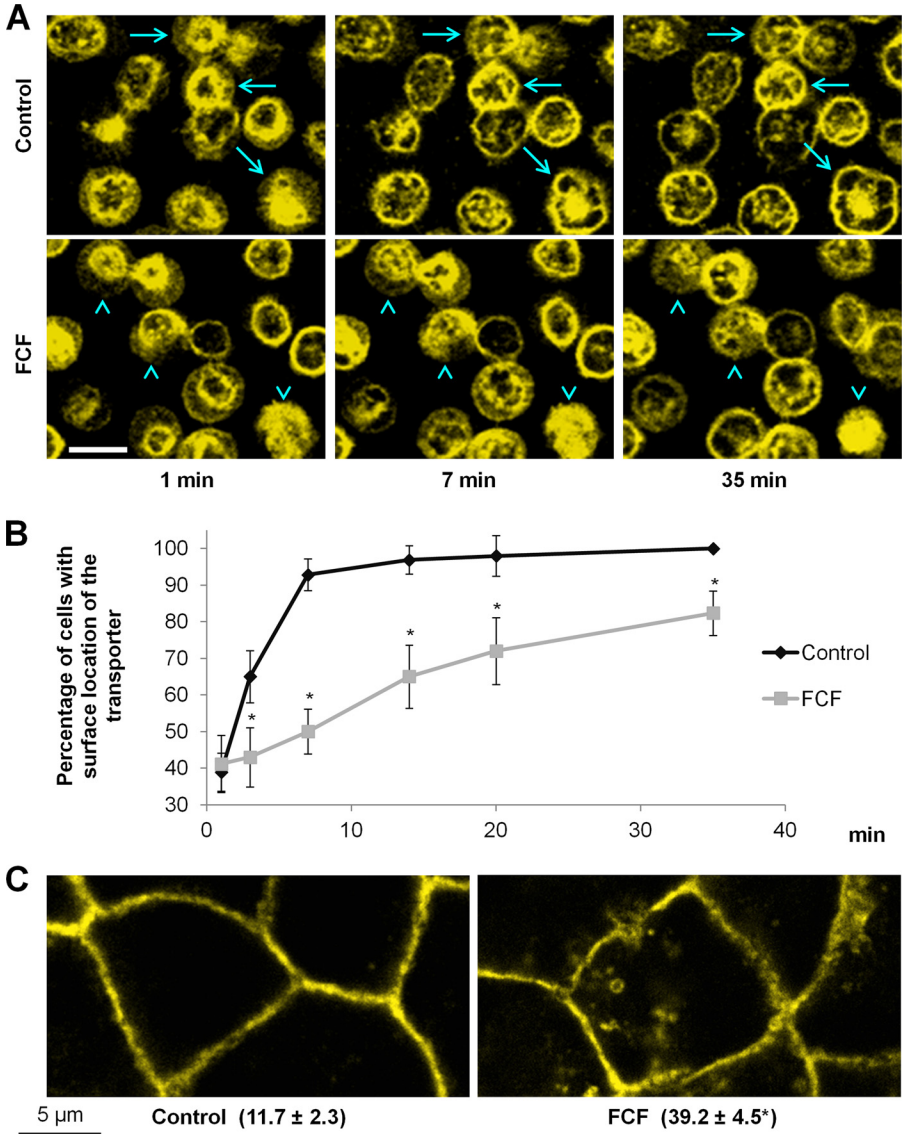

FIGURE 9. **The impairment of septin organization by FCF inhibits insertion of internalized transmembrane proteins in the plasmalemma.** MDCK cells stably expressing YFP-tagged basolateral bile acid transporter were grown in glass bottom plates until the cells formed a confluent monolayer. Cells were incubated in a Ca^{2+}-free PBS buffer for 35 min to induce internalization of the transporter. At this point, the Ca^{2+}-free PBS buffer was replaced by complete culture medium (containing Ca^{2+}) with or without 100 μM FCF, and the insertion of the internalized transporter in the plasmalemma was monitored by time lapse confocal microscopy. *A*, selected images of cells incubated with or without FCF for the indicated periods of time. The reinsertion of the transporter in the plasmalemma was attenuated in the presence of FCF as evident from the comparison of three control cells (*arrows*) with three FCF-exposed cells (*arrowheads*). *Scale bar*, 20 μm. *B*, statistical analysis of the results of the time lapse confocal microscopy experiments indicates that FCF significantly attenuates the insertion of the internalized basolateral protein in the plasmalemma. *C*, high resolution confocal microscopy images of cells incubated with or without 100 μM FCF for 2 h after replacing the Ca^{2+}-free PBS buffer with the medium. The ratio between the intracellular fluorescence intensity and the total cellular fluorescence intensity, which was calculated as described in the legend to Fig. 8, is shown below the images. *Scale bar*, 5 μm. *Error bars*, S.D. ($n = 3$ independent experiments); *, significant difference from the control, $p < 0.01$, Student's *t* test.

may differ in the pools of vesicles, the source of Ca^{2+} to trigger release, and the identity of the Ca^{2+} sensor for release but share the key SNARE-mediated fusion mechanism (59, 60). This strongly suggests that septins can modulate SNARE-mediated membrane fusion.

Septin-containing Protein Complexes Undergo Continuous Reorganization during the Exocytosis/Endocytosis Cycle—Septin-2 interacts with NSF but not with α-SNAP (Fig. 1), indicating that the interaction between septin-2 and NSF is independent of the known interactions of septin-2, septin-5, septin-4, and septin-8 with syntaxin-1 or syntaxin-4 (17, 19–22, 24). Also, septin-2 must be released from NSF prior to the formation of the NSF-SNARE complex (Fig. 12, *step 1*) and must rebind to NSF after the disassembly of the SNARE complex (Fig. 12, *step 2*). Therefore, septin-2-containing protein complexes undergo assembly and disassembly during each exocytosis/endocytosis cycle. These data are in agreement with the previously published results showing that septin-5 interacts with the NSF-free SNARE complex but not with NSF-SNARE complex (19).

Both septin-2 siRNA and impairment of septin dynamics by FCF reduce the rate of secretion of sec-β1, induce the intracellular accumulation of the post-Golgi sec-β1 carriers, do not alter the rate of the ER to Golgi trafficking (Figs. 3, 5, and 6), and

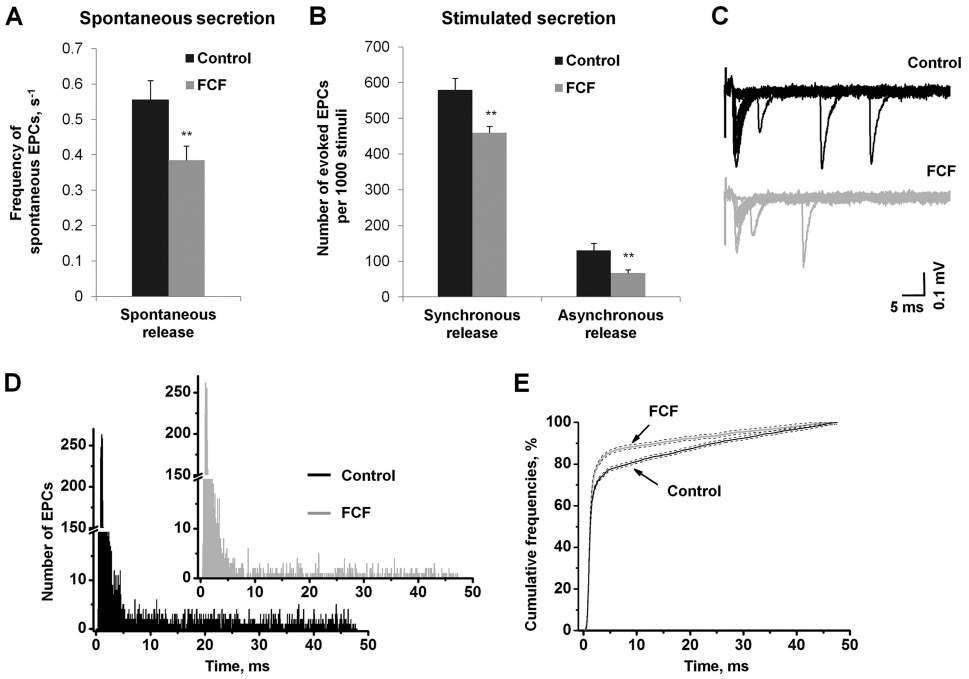

FIGURE 10. **Effect of FCF on acetylcholine secretion in mouse phrenic nerve-diaphragm muscle preparations.** *A* and *B*, effect of 20 μM FCF on spontaneous and evoked acetylcholine secretion was determined by measuring the extracellular EPCs in mouse phrenic nerve-diaphragm muscle preparations incubated with or without 20 μM FCF. Statistical analysis of the results indicates that FCF inhibits spontaneous acetylcholine secretion (*A*) and both the synchronous and delayed asynchronous components of evoked secretion (*B*). *Error bars*, S.D.; **, significant difference from the control, $p < 0.05$ ($n = 6$ mice), Student's *t* test. *C*, superposition of EPCs recorded at the synapse at 0.5-Hz stimulation frequency in control (*black lines*) and in the presence of 20 μM FCF (*gray lines*). Ten traces were superimposed, showing extracellularly recorded presynaptic nerve action potentials, individual EPCs, and stimulus artifacts. *D*, representative histogram of the distribution of synaptic delays of EPCs recorded in response to 1,000 nerve stimuli in control (*black*) and with FCF (*gray*). *E*, cumulative plots for synaptic delays in control (*black line*) and after 20 μM FCF treatment (*gray line*). The statistical significance of the difference between two cumulative curves was assessed by the Kolmogorov-Smirnov test; $p < 0.05$ was taken as significant.

increase intracellular accumulation of vesicular carriers containing transmembrane proteins (Fig. 8). These observations strongly suggest that the effects of FCF are mediated through septins, consistent with altered distribution of septin-2 and septin-9 by FCF in all cell lines used in the present study (Figs. 4, 7*C*, and 8*D*). A recent study demonstrated that FCF alters mitochondrial morphology (61). Based on this observation, the authors suggested the existence of non-septin targets of FCF, but no such targets have been identified (61). Moreover, no evidence has been presented that the morphological changes in mitochondria are independent of the FCF-induced impairment of assembly and disassembly of septins that are known to reside in mitochondria (62). Conversely, similar effects of FCF and septin silencing on various cellular processes, including mitosis and cell migration (27), protein stability (63), glucose transport (23), store-operated Ca^{2+} influx (44), ciliogenesis (47), epithelial junctions (64), gastrulation during embryogenesis (65), and bacterial invasion (66), demonstrate that FCF is a valuable tool to interfere with septin dynamics. The inhibitory effects of FCF on constitutive protein secretion, exocytosis-mediated insertion of transmembrane proteins in the plasmalemma, induced cytokine secretion, and both spontaneous and stimulated neurotransmitter release (Figs. 5–9) indicate that normal assembly and disassembly of septin oligomers is important for exocytosis of proteins (both secreted and transmembrane) and neurotransmitters.

Septins Regulate Exocytosis by Dynamically Interacting with Key Components of the Exocytosis Machinery—Our data on the importance of septin-2 and septin dynamics for the late steps of exocytosis are consistent with previously published results on the interaction of septins with the mammalian exocyst complex (13, 67, 68) and SNARE proteins (17, 19–24), which facilitate vesicle docking and fusion, respectively. Here, we demonstrated that septin-2 interacts with other key components of the exocytosis/recycling machinery (Table 1), including the chaperones that maintain functional conformation of individual SNARE proteins, Munc-18-1 that facilitates the assembly of SNARE complexes prior to membrane fusion and is important for vesicle priming, and NSF that promotes disassembly of SNARE complexes after completing the fusion event (Table 1 and Figs. 1 and 11). Each of these septin-interacting proteins is essential for exocytosis (1, 2, 5), suggesting that the impairment of all or some of these interactions by septin-2 siRNA or impairment of septin dynamics by FCF may be responsible for the observed reduction in exocytosis.

Our results demonstrate that septins are important for normal interaction of SNAP-25 with its chaperone Hsc70. The monomeric SNAP-25 is known to directly interact with the Hsc70-containing trimeric chaperone complex in neurons, and this interaction facilitates the formation of functional SNARE complexes by preventing the aggregation and degradation of the monomeric SNAP-25 (69). Here, we demonstrate that exposure of neuroendocrine cells to FCF impairs the interaction between SNAP-25 and Hsc70, reduces the total amount of SNAP-25, and decreases the resistance of SNARE complexes to dissociation by SDS (Fig. 11). Septin oligomers facilitate the interaction between SNAP-25 and its chaperones presumably by forming a membrane-associated scaffold for this protein

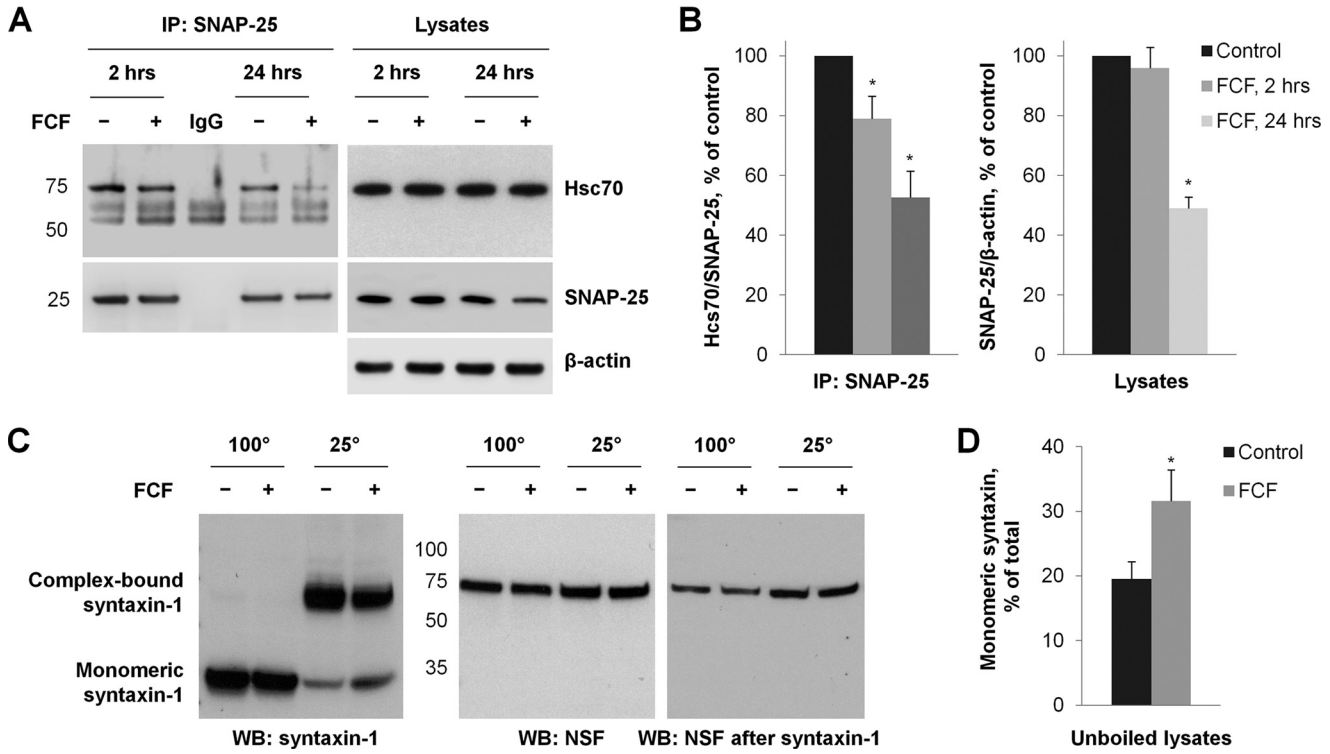

FIGURE 11. **FCF alters interactions between the components of the exocytosis machinery.** *A*, effect of FCF on co-immunoprecipitation (*IP*) of Hsc70 with SNAP-25 in PC12 cells. *B*, densitometry quantification of the results shown in *A* indicates that FCF decreases both the interaction of Hsc70 with SNAP-25 and the amount of SNAP-25 in cell lysates. *C*, Western blot (*WB*) analysis of PC12 cell lysates that were incubated at 100 °C or at room temperature in SDS-containing sample buffer for 15 min prior to loading for SDS-PAGE. The blots developed with anti-syntaxin-1 antibody were stripped and probed with anti-NSF antibody to control equal loading in unboiled samples. *D*, densitometry quantification of the unboiled samples probed with anti-syntaxin-1 antibody shown in *C* indicated that the ratio between monomeric and complex-associated syntaxin-1 was increased by FCF treatment in PC12 cells. *Error bars*, S.D. ($n = 3$ independent experiments); *, significant difference from the control, $p < 0.05$, Student's *t* test.

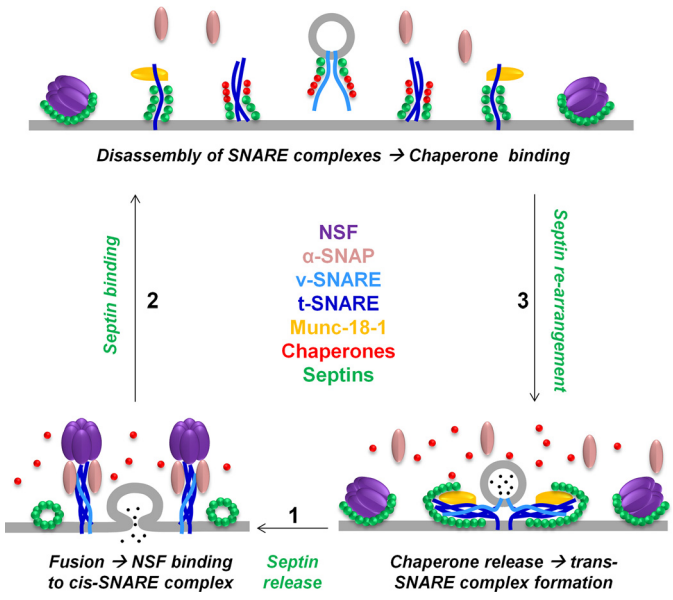

FIGURE 12. **Septin dynamics are required for exocytosis.** Septins interact with SNARE-free NSF, Munc-18-1, vesicular SNARE proteins (*v-SNARE*), plasma membrane SNARE proteins (*t-SNARE*), and their chaperones, such as synucleins and Hsc70, but not with the NSF-SNARE complex, indicating that septin oligomers undergo cycles of assembly and disassembly during exocytosis (*steps 1–3*). By interacting with proteins involved in exocytosis, septins presumably control their binding-competent positioning in the plasma membrane and/or secretory vesicles. The interaction of SNARE complexes with Munc-18-1 and NSF and the interaction of individual SNARE proteins with Munc-18-1 and chaperones are shown based on the previously published data (for a review, see Ref. 1).

complex. Disruption of normal septin polymerization by FCF impairs the interaction between monomeric SNAP-25 and Hsc70 and increases the susceptibility of SNAP-25 to degradation. The resulting decrease in the cellular levels of SNAP-25 affects the formation of SNARE complexes and inhibits exocytosis. Therefore, rearrangements of septin-containing protein complexes are important for the interaction of monomeric SNAP-25 with its chaperones (Fig. 12, *step 2*), protecting SNAP-25 from intracellular degradation and enabling normal SNARE complex formation (Fig. 12, *step 3*).

The interaction between septin-2 and NSF (Table 1 and Fig. 1) suggests that septin-2 might also be involved in regulation of the disassembly of SNARE complexes after exocytosis (Fig. 12, *step 2*). Could septins facilitate exocytosis by immobilizing the SNARE-free NSF to prevent the premature dissociation of SNARE complexes? This possibility has been ruled out because NSF silencing decreases secretion (Fig. 3). Instead, the data favor the alternative mechanism implying that septins interact separately with NSF and SNARE complexes to facilitate their localized and timely interaction in the target membrane and must be released to allow the formation of the NSF-SNARE complex (Fig. 12, *step 1*).

In conclusion, comprehensive proteomic analysis of the septin interactome followed by physiological assays in cultured cells and mouse neuromuscular junctions demonstrates that both the presence of septin-2 and dynamic reorganization of septin-containing complexes are important for the late steps of

exocytosis at the plasma membrane, such as vesicle docking to or vesicle fusion with the plasmalemma. Septins regulate exocytosis by interacting with key components of the membrane fusion machinery and facilitating their localized and timely interactions.

Acknowledgments—We thank Dr. Cameron Gundersen for fruitful discussion of the results and helpful suggestions. We thank Dr. Daniel Mènard for allowing use of the HGE-20 cell line for this work, Dr. C. L. Laboisse for providing HGT-1 cells, and Dr. Robert Lamb for providing influenza virus. We are grateful to Maura Hamrick and Liora Shoshani for providing an expression vector for the secreted extracellular domain of the dog β_1 subunit.

REFERENCES

1. Südhof, T. C., and Rizo, J. (2011) Synaptic vesicle exocytosis. *Cold Spring Harb. Perspect. Biol.* **3,** a005637
2. Südhof, T. C. (2013) Neurotransmitter release: the last millisecond in the life of a synaptic vesicle. *Neuron* **80,** 675–690
3. Han, G. A., Malintan, N. T., Collins, B. M., Meunier, F. A., and Sugita, S. (2010) Munc18-1 as a key regulator of neurosecretion. *J. Neurochem.* **115,** 1–10
4. Cipriano, D. J., Jung, J., Vivona, S., Fenn, T. D., Brunger, A. T., and Bryant, Z. (2013) Processive ATP-driven substrate disassembly by the *N*-ethylmaleimide-sensitive factor (NSF) molecular machine. *J. Biol. Chem.* **288,** 23436–23445
5. Sharma, M., Burré, J., Bronk, P., Zhang, Y., Xu, W., and Südhof, T. C. (2012) CSPα knockout causes neurodegeneration by impairing SNAP-25 function. *EMBO J.* **31,** 829–841
6. Burré, J., Sharma, M., Tsetsenis, T., Buchman, V., Etherton, M. R., and Südhof, T. C. (2010) α-Synuclein promotes SNARE-complex assembly *in vivo* and *in vitro*. *Science* **329,** 1663–1667
7. Mostowy, S., and Cossart, P. (2012) Septins: the fourth component of the cytoskeleton. *Nat. Rev. Mol. Cell Biol.* **13,** 183–194
8. Nakahira, M., Macedo, J. N., Seraphim, T. V., Cavalcante, N., Souza, T. A., Damalio, J. C., Reyes, L. F., Assmann, E. M., Alborghetti, M. R., Garratt, R. C., Araujo, A. P., Zanchin, N. I., Barbosa, J. A., and Kobarg, J. (2010) A draft of the human septin interactome. *PLoS One* **5,** e13799
9. Saarikangas, J., and Barral, Y. (2011) The emerging functions of septins in metazoans. *EMBO Rep.* **12,** 1118–1126
10. Gilden, J., and Krummel, M. F. (2010) Control of cortical rigidity by the cytoskeleton: emerging roles for septins. *Cytoskeleton* **67,** 477–486
11. He, B., and Guo, W. (2009) The exocyst complex in polarized exocytosis. *Curr. Opin. Cell Biol.* **21,** 537–542
12. Hsu, S. C., Hazuka, C. D., Foletti, D. L., and Scheller, R. H. (1999) Targeting vesicles to specific sites on the plasma membrane: the role of the sec6/8 complex. *Trends Cell Biol.* **9,** 150–153
13. Hsu, S. C., Hazuka, C. D., Roth, R., Foletti, D. L., Heuser, J., and Scheller, R. H. (1998) Subunit composition, protein interactions, and structures of the mammalian brain sec6/8 complex and septin filaments. *Neuron* **20,** 1111–1122
14. Tsang, C. W., Estey, M. P., DiCiccio, J. E., Xie, H., Patterson, D., and Trimble, W. S. (2011) Characterization of presynaptic septin complexes in mammalian hippocampal neurons. *Biol. Chem.* **392,** 739–749
15. Xue, J., Tsang, C. W., Gai, W. P., Malladi, C. S., Trimble, W. S., Rostas, J. A., and Robinson, P. J. (2004) Septin 3 (G-septin) is a developmentally regulated phosphoprotein enriched in presynaptic nerve terminals. *J. Neurochem.* **91,** 579–590
16. Yang, Y. M., Fedchyshyn, M. J., Grande, G., Aitoubah, J., Tsang, C. W., Xie, H., Ackerley, C. A., Trimble, W. S., and Wang, L. Y. (2010) Septins regulate developmental switching from microdomain to nanodomain coupling of Ca^{2+} influx to neurotransmitter release at a central synapse. *Neuron* **67,** 100–115
17. Ihara, M., Yamasaki, N., Hagiwara, A., Tanigaki, A., Kitano, A., Hikawa, R., Tomimoto, H., Noda, M., Takanashi, M., Mori, H., Hattori, N., Miyakawa, T., and Kinoshita, M. (2007) Sept4, a component of presynaptic scaffold and Lewy bodies, is required for the suppression of α-synuclein neurotoxicity. *Neuron* **53,** 519–533
18. Kinoshita, A., Noda, M., and Kinoshita, M. (2000) Differential localization of septins in the mouse brain. *J. Comp. Neurol.* **428,** 223–239
19. Beites, C. L., Campbell, K. A., and Trimble, W. S. (2005) The septin Sept5/CDCrel-1 competes with α-SNAP for binding to the SNARE complex. *Biochem. J.* **385,** 347–353
20. Beites, C. L., Xie, H., Bowser, R., and Trimble, W. S. (1999) The septin CDCrel-1 binds syntaxin and inhibits exocytosis. *Nat. Neurosci.* **2,** 434–439
21. Amin, N. D., Zheng, Y. L., Kesavapany, S., Kanungo, J., Guszczynski, T., Sihag, R. K., Rudrabhatla, P., Albers, W., Grant, P., and Pant, H. C. (2008) Cyclin-dependent kinase 5 phosphorylation of human septin SEPT5 (hCDCrel-1) modulates exocytosis. *J. Neurosci.* **28,** 3631–3643
22. Ito, H., Atsuzawa, K., Morishita, R., Usuda, N., Sudo, K., Iwamoto, I., Mizutani, K., Katoh-Semba, R., Nozawa, Y., Asano, T., and Nagata, K. (2009) Sept8 controls the binding of vesicle-associated membrane protein 2 to synaptophysin. *J. Neurochem.* **108,** 867–880
23. Wasik, A. A., Polianskyte-Prause, Z., Dong, M. Q., Shaw, A. S., Yates, J. R., 3rd, Farquhar, M. G., and Lehtonen, S. (2012) Septin 7 forms a complex with CD2AP and nephrin and regulates glucose transporter trafficking. *Mol. Biol. Cell* **23,** 3370–3379
24. Dent, J., Kato, K., Peng, X. R., Martinez, C., Cattaneo, M., Poujol, C., Nurden, P., Nurden, A., Trimble, W. S., and Ware, J. (2002) A prototypic platelet septin and its participation in secretion. *Proc. Natl. Acad. Sci. U.S.A.* **99,** 3064–3069
25. Ono, R., Ihara, M., Nakajima, H., Ozaki, K., Kataoka-Fujiwara, Y., Taki, T., Nagata, K., Inagaki, M., Yoshida, N., Kitamura, T., Hayashi, Y., Kinoshita, M., and Nosaka, T. (2005) Disruption of Sept6, a fusion partner gene of MLL, does not affect ontogeny, leukemogenesis induced by MLL-SEPT6, or phenotype induced by the loss of Sept4. *Mol. Cell. Biol.* **25,** 10965–10978
26. Tsang, C. W., Fedchyshyn, M., Harrison, J., Xie, H., Xue, J., Robinson, P. J., Wang, L. Y., and Trimble, W. S. (2008) Superfluous role of mammalian septins 3 and 5 in neuronal development and synaptic transmission. *Mol. Cell. Biol.* **28,** 7012–7029
27. Hu, Q., Nelson, W. J., and Spiliotis, E. T. (2008) Forchlorfenuron alters mammalian septin assembly, organization, and dynamics. *J. Biol. Chem.* **283,** 29563–29571
28. Iwase, M., Okada, S., Oguchi, T., and Toh-e, A. (2004) Forchlorfenuron, a phenylurea cytokinin, disturbs septin organization in *Saccharomyces cerevisiae*. *Genes Genet. Syst.* **79,** 199–206
29. DeMay, B. S., Meseroll, R. A., Occhipinti, P., and Gladfelter, A. S. (2010) Cellular requirements for the small molecule forchlorfenuron to stabilize the septin cytoskeleton. *Cytoskeleton* **67,** 383–399
30. Angelis, D., Karasmanis, E. P., Bai, X., and Spiliotis, E. T. (2014) *In silico* docking of forchlorfenuron (FCF) to septins suggests that FCF interferes with GTP binding. *PLoS One* **9,** e96390
31. Carmosino, M., Procino, G., Casavola, V., Svelto, M., and Valenti, G. (2000) The cultured human gastric cells HGT-1 express the principal transporters involved in acid secretion. *Pflugers Arch.* **440,** 871–880
32. Doné, S. C., Leibiger, I. B., Efendiev, R., Katz, A. I., Leibiger, B., Berggren, P. O., Pedemonte, C. H., and Bertorello, A. M. (2002) Tyrosine 537 within the Na^+,K^+-ATPase α-subunit is essential for AP-2 binding and clathrin-dependent endocytosis. *J. Biol. Chem.* **277,** 17108–17111
33. Vagin, O., Tokhtaeva, E., and Sachs, G. (2006) The role of the β1 subunit of the Na,K-ATPase and its glycosylation in cell-cell adhesion. *J. Biol. Chem.* **281,** 39573–39587
34. Chailler, P., and Ménard, D. (2005) Establishment of human gastric epithelial (HGE) cell lines exhibiting barrier function, progenitor, and prezymogenic characteristics. *J. Cell. Physiol.* **202,** 263–274
35. Tokhtaeva, E., Sachs, G., and Vagin, O. (2010) Diverse pathways for maturation of the Na,K-ATPase β1 and β2 subunits in the endoplasmic reticulum of Madin-Darby canine kidney cells. *J. Biol. Chem.* **285,** 39289–39302
36. Tokhtaeva, E., Clifford, R. J., Kaplan, J. H., Sachs, G., and Vagin, O. (2012) Subunit isoform selectivity in assembly of Na,K-ATPase α-β

heterodimers. *J. Biol. Chem.* **287,** 26115–26125
37. Padilla-Benavides, T., Roldán, M. L., Larre, I., Flores-Benitez, D., Villegas-Sepúlveda, N., Contreras, R. G., Cereijido, M., and Shoshani, L. (2010) The polarized distribution of Na^+,K^+-ATPase: role of the interaction between β subunits. *Mol. Biol. Cell* **21,** 2217–2225
38. Tokhtaeva, E., Sachs, G., Sun, H., Dada, L. A., Sznajder, J. I., and Vagin, O. (2012) Identification of the amino acid region involved in the intercellular interaction between the β1 subunits of Na^+/K^+-ATPase. *J. Cell Sci.* **125,** 1605–1616
39. Rappsilber, J., Mann, M., and Ishihama, Y. (2007) Protocol for micro-purification, enrichment, pre-fractionation and storage of peptides for proteomics using StageTips. *Nat. Protoc.* **2,** 1896–1906
40. Brigant, J. L., and Mallart, A. (1982) Presynaptic currents in mouse motor endings. *J. Physiol.* **333,** 619–636
41. Bukcharaeva, E. A., Kim, K. C., Moravec, J., Nikolsky, E. E., and Vyskocil, F. (1999) Noradrenaline synchronizes evoked quantal release at frog neuromuscular junctions. *J. Physiol.* **517,** 879–888
42. Katz, B., and Miledi, R. (1965) The measurement of synaptic delay, and the time course of acetylcholine release at the neuromuscular junction. *Proc. R. Soc. Lond. B Biol. Sci.* **161,** 483–495
43. Bukharaeva, E. A., Samigullin, D., Nikolsky, E. E., and Magazanik, L. G. (2007) Modulation of the kinetics of evoked quantal release at mouse neuromuscular junctions by calcium and strontium. *J. Neurochem.* **100,** 939–949
44. Sharma, S., Quintana, A., Findlay, G. M., Mettlen, M., Baust, B., Jain, M., Nilsson, R., Rao, A., and Hogan, P. G. (2013) An siRNA screen for NFAT activation identifies septins as coordinators of store-operated Ca^{2+} entry. *Nature* **499,** 238–242
45. Tooley, A. J., Gilden, J., Jacobelli, J., Beemiller, P., Trimble, W. S., Kinoshita, M., and Krummel, M. F. (2009) Amoeboid T lymphocytes require the septin cytoskeleton for cortical integrity and persistent motility. *Nat. Cell Biol.* **11,** 17–26
46. Kremer, B. E., Haystead, T., and Macara, I. G. (2005) Mammalian septins regulate microtubule stability through interaction with the microtubule-binding protein MAP4. *Mol. Biol. Cell* **16,** 4648–4659
47. Ghossoub, R., Hu, Q., Failler, M., Rouyez, M. C., Spitzbarth, B., Mostowy, S., Wolfrum, U., Saunier, S., Cossart, P., Jamesnelson, W., and Benmerah, A. (2013) Septins 2, 7 and 9 and MAP4 colocalize along the axoneme in the primary cilium and control ciliary length. *J. Cell Sci.* **126,** 2583–2594
48. Naydenov, N. G., Harris, G., Brown, B., Schaefer, K. L., Das, S. K., Fisher, P. B., and Ivanov, A. I. (2012) Loss of soluble *N*-ethylmaleimide-sensitive factor attachment protein α (αSNAP) induces epithelial cell apoptosis via down-regulation of Bcl-2 expression and disruption of the Golgi. *J. Biol. Chem.* **287,** 5928–5941
49. Gerlach, R. L., Camp, J. V., Chu, Y. K., and Jonsson, C. B. (2013) Early host responses of seasonal and pandemic influenza A viruses in primary well-differentiated human lung epithelial cells. *PLoS One* **8,** e78912
50. Stanley, A. C., and Lacy, P. (2010) Pathways for cytokine secretion. *Physiology* **25,** 218–229
51. Takeuchi, O., and Akira, S. (2010) Pattern recognition receptors and inflammation. *Cell* **140,** 805–820
52. Müsch, A. (2004) Microtubule organization and function in epithelial cells. *Traffic* **5,** 1–9
53. Spiliotis, E. T. (2010) Regulation of microtubule organization and functions by septin GTPases. *Cytoskeleton* **67,** 339–345
54. Ageta-Ishihara, N., Miyata, T., Ohshima, C., Watanabe, M., Sato, Y., Hamamura, Y., Higashiyama, T., Mazitschek, R., Bito, H., and Kinoshita, M. (2013) Septins promote dendrite and axon development by negatively regulating microtubule stability via HDAC6-mediated deacetylation. *Nat. Commun.* **4,** 2532
55. Spiliotis, E. T., Hunt, S. J., Hu, Q., Kinoshita, M., and Nelson, W. J. (2008) Epithelial polarity requires septin coupling of vesicle transport to polyglutamylated microtubules. *J. Cell Biol.* **180,** 295–303
56. Bowen, J. R., Hwang, D., Bai, X., Roy, D., and Spiliotis, E. T. (2011) Septin GTPases spatially guide microtubule organization and plus end dynamics in polarizing epithelia. *J. Cell Biol.* **194,** 187–197
57. Cole, N. B., Sciaky, N., Marotta, A., Song, J., and Lippincott-Schwartz, J. (1996) Golgi dispersal during microtubule disruption: regeneration of Golgi stacks at peripheral endoplasmic reticulum exit sites. *Mol. Biol. Cell* **7,** 631–650
58. Rizzoli, S. O. (2014) Synaptic vesicle recycling: steps and principles. *EMBO J.* **33,** 788–822
59. Kaeser, P. S., and Regehr, W. G. (2014) Molecular mechanisms for synchronous, asynchronous, and spontaneous neurotransmitter release. *Annu. Rev. Physiol.* **76,** 333–363
60. Smith, S. M., Chen, W., Vyleta, N. P., Williams, C., Lee, C. H., Phillips, C., and Andresen, M. C. (2012) Calcium regulation of spontaneous and asynchronous neurotransmitter release. *Cell Calcium* **52,** 226–233
61. Heasley, L. R., Garcia, G., 3rd, and McMurray, M. A. (2014) Off-target effects of the "septin drug" forchlorfenuron in non-plant eukaryotes. *Eukaryot. Cell* **13,** 1411–1420
62. Mandel-Gutfreund, Y., Kosti, I., and Larisch, S. (2011) ARTS, the unusual septin: structural and functional aspects. *Biol. Chem.* **392,** 783–790
63. Vagin, O., Tokhtaeva, E., Garay, P. E., Souda, P., Bassilian, S., Whitelegge, J. P., Lewis, R., Sachs, G., Wheeler, L., Aoki, R., and Fernandez-Salas, E. (2014) Recruitment of septin cytoskeletal proteins by botulinum toxin A protease determines its remarkable stability. *J. Cell Sci.* **127,** 3294–3308
64. Sidhaye, V. K., Chau, E., Breysse, P. N., and King, L. S. (2011) Septin-2 mediates airway epithelial barrier function in physiologic and pathologic conditions. *Am. J. Respir. Cell Mol. Biol.* **45,** 120–126
65. Kim, S. K., Shindo, A., Park, T. J., Oh, E. C., Ghosh, S., Gray, R. S., Lewis, R. A., Johnson, C. A., Attie-Bittach, T., Katsanis, N., and Wallingford, J. B. (2010) Planar cell polarity acts through septins to control collective cell movement and ciliogenesis. *Science* **329,** 1337–1340
66. Mostowy, S., Danckaert, A., Tham, T. N., Machu, C., Guadagnini, S., Pizarro-Cerdá, J., and Cossart, P. (2009) Septin 11 restricts InlB-mediated invasion by *Listeria*. *J. Biol. Chem.* **284,** 11613–11621
67. Rittmeyer, E. N., Daniel, S., Hsu, S. C., and Osman, M. A. (2008) A dual role for IQGAP1 in regulating exocytosis. *J. Cell Sci.* **121,** 391–403
68. Vega, I. E., and Hsu, S. C. (2003) The septin protein Nedd5 associates with both the exocyst complex and microtubules and disruption of its GTPase activity promotes aberrant neurite sprouting in PC12 cells. *Neuroreport* **14,** 31–37
69. Sharma, M., Burré, J., and Südhof, T. C. (2011) CSPα promotes SNARE-complex assembly by chaperoning SNAP-25 during synaptic activity. *Nat. Cell Biol.* **13,** 30–39